Assessment of rainwater runoff using the Rational Method and its applications

Applied to rural case studies in Ockelbo, Sweden, affected by the extreme rain event in Gävleborg county of August 2021

Master's Thesis in Master Program Infrastructure and Environmental Engineering

ANNIE DRISTIG

ELIN VÄLIKANGAS

Department of Architecture and Civil Engineering
CHALMERS UNIVERSITY OF TECHNOLOGY
Master's Thesis ACEX30
Gothenburg, Sweden 2022

MASTER'S THESIS ACEX30

Assessment of rainwater runoff using the Rational Method and its applications

Applied to rural case studies in Ockelbo, Sweden, affected by the extreme rain event in Gävleborg county of August 2021

Master's Thesis in Master Program Infrastructure and Environmental Engineering

ANNIE DRISTIG
ELIN VÄLIKANGAS

Department of Architecture and Civil Engineering
Division of Water Environment Technology
CHALMERS UNIVERSITY OF TECHNOLOGY
Gothenburg, Sweden 2022

Assessment of rainwater runoff using the Rational Method and its applications
Applied to rural case studies in Ockelbo, Sweden, affected by the extreme rain event in Gävleborg county of August 2021

Master's Thesis in Master Program Infrastructure and Environmental Engineering
ANNIE DRISTIG
ELIN VÄLIKANGAS

Supervisors:
Adjunct Professor Yvonne Andersson-Sköld, Department of Architecture and Civil Engineering, Division of Geology and Geotechnics, Chalmers University of Technology, Gothenburg
Geotechnician Agne Gunnarsson, Swedish Transport Administration, Linköping

Examiner:
Professor Sebastien Rauch, Department of Architecture and Civil Engineering, Division of Water Environment Technology, Chalmers University of Technology, Gothenburg

Department of Architecture and Civil Engineering
Division of Water Environment Technology
Chalmers University of Technology
SE-412 96 Gothenburg
Telephone +46 31 772 1000

Cover: The collapse of a culvert pipe in Ockelbo, Sweden, due to *"Gävleregnet"* in August 2021. Reprinted with permission from P4 Gävleborg/Sveriges Radio (2021).

Department of Architecture and Civil Engineering
Gothenburg, Sweden 2022

Assessment of rainwater runoff using the Rational Method and its applications
Applied to rural case studies in Ockelbo, Sweden, affected by the extreme rain event in Gävleborg county of August 2021
ANNIE DRISTIG
ELIN VÄLIKANGAS
Department of Water Environment Technology
Chalmers University of Technology

Abstract

The aim of this master thesis is to investigate different applications of the Rational Method (RM), applied to manually calculate rainwater runoff and estimate culvert pipe dimensions at two rural case study areas affected by the extreme rainfall in Gävleborg county in August 2021. This rain event is in Sweden referred to as *Gävleregnet*. Each case study consisted of a culvert pipe transporting a creek through a country road. The dimensioning flows from the forested catchment areas were calculated by the RM and three of its applications; the version of Svenskt Vatten (SV-RM), the Swedish Transport Administration (STA-RM) and *Flödesappen*. All of these except the latter, which is a digital modelling tool, were combined with the Time-area Method (T-A), and their calculations were based on two rain scenarios; the Worst Case of Intensity (WCI) and the Worst Case of Return Period (WCRP). All four applications of the RM utilized Colebrook's method to determine the suitable pipe dimensions needed to manage the dimensioning flows. Furthermore, the catchment areas and calculations for RM, SV-RM and STA-RM were estimated manually in Excel and GIS. A field visit was also conducted to retrieve deepened information of the case study areas. The results of the areal parameters were compared between the digital calculation in *Flödesappen* and the manual methods. The influence of some parameters on the peak flow was investigated in a Sensitivity Analysis (SA) for each method and rain scenario.

Overall, the results showed that the WCRP was the actual worst of the two scenarios, for both case studies, where the highest peak flows were generated by the two methods that considered a climate factor (SV-RM and STA-RM). The results from the SA show that the most affected flow is generated by the change of the catchment area in the WCRP scenario for SV-RM and STA-RM.

Keywords: Rational Method, Time-area method, Culvert pipe, Runoff, Swedish Transport Administration, Svenskt Vatten, Gävleregnet, Extreme rain event, Rural, Catchment area.

Acknowledgements

First of all, we thank our wonderful supervisors, Yvonne Andersson-Sköld from Chalmers University of Technology/VTI and Agne Gunnarsson from the Swedish Transport Administration for all of your time and commitment during our work. Performing this thesis would not have been as rewarding and fun without your guidance and support. Also, a special thanks to our examiner Sebastien Rauch and professor Thomas Pettersson from Chalmers University of Technology for your feedback and interest in our work.

From the Swedish Transport Administration, we also want to direct our gratitude to Klas Hansson for sharing his expertise in hydrology, and to Zeljko Simunovic for always lending a hand in GIS-related matter and showing us his kindness. To Håkan Nordlander, Stefan Styffe and Magnus Billberger, a special thanks for helping us developing the aim and focus of this thesis. And thank you to Britt-Marie Nilsson and Magnus Granados Huldén who helped us with all administrative but equally issues.

From Chalmers University of Technology, we thank Fia Börjesson and Carl-Johan Carlsson for taking their time and guiding us in scientific writing at the beginning of the work.

Finally, we express our thankfulness to Magnus Westerstrand from Gävle municipality who has provided us with valuable precipitation data, and to Lina Nordin from VTI who has been involved and guided us during our supervisor meetings.

Annie Dristig & Elin Välikangas, Gothenburg, June 2022

Contents

List of Figures

List of Tables

Terminology

The following terminology explains some concepts and acronyms that have been used throughout this thesis, listed in alphabetical order:

Catchment area	An area of which the water is drained to a watercourse upstream of a specific point. The area is usually limited by ridges/water dividers, which divide the flow from precipitation etc. in different directions.
Concentration time	The time equal to when the whole catchment area contributes to the runoff flow (see *Runoff*) in a specific point, expressed in minutes.
Culvert pipe	A structural element that enables stormwater and/or streams to pass unhindered under a road and through its embankment. The material is usually concrete, steel or plastic. The element has a theoretical diameter of up to 2 meters inclusive, according to County Administration of Örebro (2003). Greater diameters are considered as bridges.
Gaining stream	When a stream or creek gains water flow from ground water seeping through the creek bed. The process is due to a higher water table in an adjacent coherent geological mass than the water table of the stream.
Flödesappen	*(English. the Flow application).* A program under development at the Swedish Traffic Administration. It was refined to calculate precipitation runoff in rural areas.
GIS	An acronym for Geographical Information System. A computer-based system used to analyse stored geographic data.
Gävleregnet	*(English. the Gävle rain).* An extreme rainfall that occurred in the central parts of Sweden in August 2021.

IDF	An acronym for Intensity-Duration-Frequency. A relationship that is unique to each specific rain, and is often described as a plot.
Return period	A parameter that in years describes at what recurrence rate a special or specific weather event will take place.
RM	Acronym for the Rational Method *(Swedish. Rationella Metoden)*. Further described in Chapter 2.
Runoff	The amount of precipitation left to flow on surfaces after eventual infiltration, evapotranspiration and replenishment of water bodies.
Runoff coefficient	A parameter that describes at what extent that water that originates from precipitation will contribute to runoff. The factor is a value between 0 and 1, where great permeability and/or storage capacity are closer to 0 and paved surfaces with low infiltration capabilities, closer to 1.
SCALGO Live	A program/company that utilizes 3D elevation models to simulate flooding events by seawater rise and rain scenarios.
SMHI	Acronym for the Swedish Meteorological and Hydrological Institute. A swedish state authority with expertise in hydrology and meteorology, specializing in forecasting weather, climate and environment.
STA	Acronym for the Swedish Transport Administration *(Swedish. Trafikverket)*. A state authority in charge of planning, construction, operation and maintenance of state road networks and railways in Sweden.
STA-RM	Acronym for STA's version of RM. Further described in Chapter 2.
Stigfinnaren	*(English. the Path finder)*. A web-based GIS program by the Swedish Transport Administration that makes its general knowledge accessible for the whole administration
Svenskt Vatten	*(English. Swedish Water)*. A swedish industry organization that gives out guide-lining documents to the water and wastewater industry.
SV	Acronym for Svenskt Vatten.

SV-RM	Acronym for SV's version of RM. Further described in Chapter 2.
Trenchcoat	A combination of a conventional steel culvert pipe with a plastic polymer coating. The coating protects the corrosion prone steel.
Truminventeringsappen	*(English. the Culvert pipe inventory application).* An application developed by the Swedish Transport Administration that is connected to a GIS-platform which allows users to inventory culvert pipes on their phones while they are out in the field. Holds data on placing, size and material, among others.
Vintersidan	*(English. the Winter page).* A web-page that collects all information available for the operational manager to safely maintain the roads during the winter year. The page holds information from the VViS stations and more.
VViS	An acronym for Vägväderinformationssystem *(English. Road Weather information System).* A system collecting weather data for the Swedish Transport Administration.

1
Introduction

As climate change is constantly ongoing, more intense amounts of precipitation are expected to wash through cities and rural areas (Swedish Council of Experts on Climate Adaptation, 2022), which puts pressure on the existing infrastructure for managing stormwater and rainwater runoff (Andersson-Sköld et al., 2021). In recent times, the stormwater quality has been a hot topic for researchers. But, with a rising impact from climate change, the management of increased flows is becoming increasingly important (Swedish Council of Experts on Climate Adaptation, 2022). A conclusion can therefore be drawn that the dimensioning of stormwater infrastructure is going to be more highly considered in the near future. Accordingly, in order to protect socially important functions and activities from the stresses of a changing climate, risk analyses and calculations of water flows constitute a significant part of today's preventive work and climate adaptation (Lindeberg et al., 2019).

Heavy or prolonged rain events can cause many problems, including flooding, erosion and washed away road structures (Lindeberg et al., 2019), which in turn can entail both social, economic as well as ecological damages and costs. The underlying factors can be several and interact with each other, but undersizing, misplacement or lack of maintenance of stormwater infrastructure are some of the reasons behind this. Culvert pipes are one of the most commonly used infrastructures for transporting runoff through roads and surfaces to prevent flooding and create a safe environment for transport and living (County Administration of Örebro, 2003; Andersson-Sköld et al., 2021). Furthermore, culvert pipes have for a long time been designed to withstand rain with a 50 or 100-year return period depending on the placement and the safety class of the road. It is possible that the road drainage will be designed for even greater return time periods in the future, which will leave the infrastructure of today dated and under-dimensioned.

As the Swedish Council of Experts on Climate Adaptation (2022) mentioned in their first report, the climate adaption in Sweden is in a developing phase, but much more needs to be done by all responsible stakeholders. This includes municipalities, regions, national authorities, county administrative boards and other involved actors. In agreement with this, the Swedish Transport Administration has begun a national inventory of culvert pipes to create an outline of their condition. The inventory reports, for example, the material and functional status of each pipe as well as its geographical location and pipe dimension. Furthermore, the Swedish Transport Administration maintains over 100 000 km of roads and annually spends billions of SEK maintaining the transport infrastructure (STA, 2019). The large infrastructure system naturally adds a towering number of culvert pipes in the country and the inventory has made the stock searchable, which is a huge benefit for further planning and development.

A general and well-used method for predicting stormwater flows is the Rational Method (RM), which has formed the basis for rough estimations of flow calculations since the middle of the 19th century Chin (2018). Although the basis and theory have been the same since then, the RM has been adapted with regards to deepened understanding as knowledge, technology and climate have been developed and changed over the years. Today, there are several different versions of the RM that can be used for dimensioning of stormwater flows and design of culvert pipes, including applications according to Svenskt Vatten and the Swedish Transport Administration (SV, 2016; STA, 2017). Apart from RM, there is an even greater offerings in computer-based programs. In the jungle of these methods and programs, there is a pent-up need for comparative reviews that can highlight their qualities and limitations.

In August of 2021, a heavy rainfall hit the city of Gävle and Gävleborg County in the central parts of Sweden. Within and around the county, infrastructure was either disabled or destroyed, and due to its resistance and intensity, the rainfall was considered as an extreme rain event with an unusually long return period. This report will investigate the rainwater runoff induced by this extreme rain event called *Gävleregnet*, for two rural case studies in Ockelbo municipality. More specifically, this thesis will investigate if the RM and its applications as rough estimation methods still could give an acceptable prediction of rural rainwater runoff despite its limitations.

1.1 Aim

The aim of this master thesis is to investigate different versions and applications of the Rational Method (RM), applied to manually calculate rainwater runoff and estimate culvert pipe dimensions for two rural case study areas affected by the extreme rainfall in Gävleborg county of August 2021. This rain event is in Sweden referred to as *Gävleregnet*. The work will be performed in collaboration with the Swedish Transport Administration. The ambition with this thesis is to compare and discuss the calculated results and their uncertainties, as well as to bring clarity to advantages and limitations of assessing runoff flows by the applied methods. Furthermore, the hope is that both students and stakeholders in water infrastructure industry will understand and benefit from the outcome of the work.

To fulfill the aim, the following objectives are valid for this thesis:

- Investigate RM versions and their limitations.

- Calculate the peak flows of the studied worst case rainfall scenarios applied to each case study and its corresponding culvert pipe dimension, for each method.

- Analyse and compare the results of the different applications of the RM. Discuss the manual calculations versus computer modelling, and perform a sensitivity analysis to investigate which parameters have a greater impact on the manually calculated results.

- Discuss the uncertainties regarding the weather and climate that could have affected the results of this thesis.

Based on these objectives, the research questions of this thesis are:

1. What were the estimated maximum peak flows of *Gävleregnet* in August 2021 for the two case studies, and what pipe dimensions were desired to manage these flows?

2. According to the the sensitivity analysis, which parameters have the largest impact on the calculated results?

1.2 Limitations

This thesis has been limited to investigate the following flow calculation and dimensioning methods:

- Rational Method (RM)
- Versions and applications of the RM
  - P110 by *Svenskt Vatten* (SV), referred to as SV-RM in this thesis
  - MB310 and TRVINFRA by the Swedish Transport Administration (STA), referred to as STA-RM in this thesis
  - *Flödesappen* by the STA
  - Time-area Method (T-A)
- Colebrook's method

These methods are tested against two case studies to assess their accuracy but also to be compared against each other. Limitations in terms of assumptions made in the assessment and calculation processes are described in Chapter 4.

1.3 Methodology

Initially in this thesis, a theory study was conducted to gather theoretical information about the chosen methods as a basis to rely on for the calculation and modelling of the case studies. The theory study considered reports and books that comprehensively describes each application of the RM, where three main sources were used: Lyngfelt (1981) for the RM itself, SV (2016) for the SV-RM version, STA (2017) for the STA-RM version and Lindeberg et al. (2019) for *Flödesappen*.

Programs and data banks that are available within the Swedish Transport Administration intranet have been utilized, including *Stigfinnaren, Vintersidan* and *Truminventeringsappen.* These programs made it possible to locate roads and culvert pipes that have been exposed to flooding in recent years. The criteria for the selection of the studied culvert pipes and weather event were:

- Data of the case study before the rain incident was available.
- The case study was affected by *Gävleregnet* of 2021.
- Two adjacent case studies within the Gävleborg county.

Manual calculations in Excel and modelling in *Flödesappen* were thereafter made, and the calculation processes are further described in Chapter *4 Methodology of the calculation process.*

2

Theory

The following chapter aims to describe the theory on which this thesis is based. The first Section 2.1 describes the Rational Method (RM) and its applications. In Section 2.2, the Colebrook's method of dimensioning culvert pipes is declared, and in Section 2.3 different methods for retrieving weather data are stated.

2.1 Applications of the Rational Method

As the RM has been applied for a long time without any major changes, some refined versions have been developed. The Subsections 2.1.1 - 2.1.3 describe the RM in its original form and as a version according to *Svenskt Vatten* (SV-RM) and the Swedish Transport Administration (STA-RM). A description of the so-called Time-area method (T-A) and the modelling tool *Flödesappen*, which both involve the RM, is given in Subsection 2.1.4 and 2.1.5 respectively.

2.1.1 Rational Method

The RM is a statistical method developed for calculation of peak flows of stormwater runoff in urban areas (Lyngfelt, 1981; Chin, 2018). Even though the method was developed for urban areas, it can be used to predict runoff in rural areas as well (STA, 2017). It is a functional method for dimensioning stormwater management systems that has been widely applied since the mid nineteenth century (Chin, 2018). Thus, the RM has stayed unchanged and been applied by generations of engineers for over 150 years. As more advanced methods and understanding have been further developed during this time, the conventional RM should be seen as a standard method for an initial dimensioning or first estimates of stormwater pipes because of its rough simplifications (Lyngfelt, 1981).

At the time when the entire catchment area participates in the runoff, the maximal discharge flow is attained (Lyngfelt, 1981). This specific time factor, named the concentration time (t_c), is theoretically described as the time needed for the water to flow from the most remote location to the outflow of the system. It could furthermore be regarded as a site-specific parameter since it is deeply dependent on the size, gradient and shape of the catchment area.

As more intense precipitation implies increasing flows and thus increasing water velocities on surfaces and in pipes, the rainfall intensity (i) also affects how the concentration time varies in the catchment area (Lyngfelt, 1981). This parameter depicts the hydrological properties of the area and can either be empirically calculated in several different ways, or decided from intensity-duration-frequency (IDF) plots. Such plots are based on the duration (t_r) and return period (T) of the rain. Figure 2.1 exemplifies what an IDF plot may look like, in this case based on statistically measured national data of annual average precipitation between 1995-2008 according to SMHI (2009).

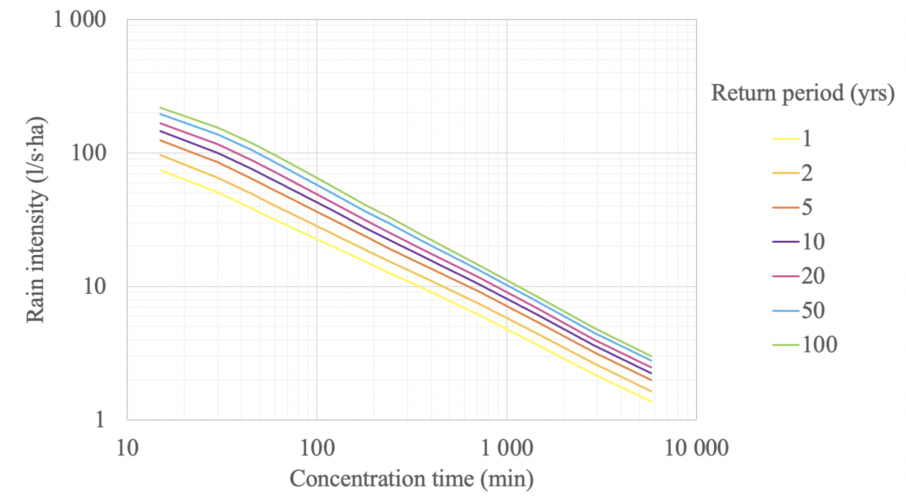

Figure 2.1: *The rain intensity for different return periods and concentration times (IDF plot). Data is a national corrected mean retrieved from SMHI (2009). Authors' own figure.*

In the RM, the duration of the rain is assumed to be equal to the concentration time of the catchment area ($t_r = t_c$), which means that the intensity becomes constant over the time required to reach the maximum catchment runoff flow. Consequently, in order to determine that constant value, the varying intensity of the rain over the determined time interval is defined as the mean intensity of this interval. The definition of combining the duration and intensity in this way, called block rain, can be used for one or more individual rain events, i.e. as a single block rain or as a series of block rain.

The runoff coefficient (φ) is a hydraulic parameter describing the rate proportionality between rainfall and runoff in the catchment area (Chin, 2018; Dhakal et al., 2013; Lyngfelt, 1981). Within RM, this ratio is assumed to be constant under the assumptions that the duration of precipitation either reaches or exceeds the concentration time of the catchment area, and that the rainfall intensity remains constant (Chin, 2018). The precipitation is also inferred to be uniformly distributed over the entire catchment area. Due to these assumptions of spatial uniformity regarding rainfall and runoff, the method is most suitable to portray medium to small catchment areas, less than 80 ha (Chin, 2018), as well as evenly distributed ones with regards to different land types (Lyngfelt, 1981). In total, valid assumptions of the RM can be listed as follows:

1. The dimensioning flow has the same return period as the rain intensity, and is reached when the entire catchment area contributes to the runoff (Lyngfelt, 1981; Chin, 2018).
2. The precipitation is uniform throughout the catchment area, and both the rainfall rate and the ratio between runoff and rainfall is constant (Chin, 2018).
3. The runoff coefficient integrates all rainfall abstractions (Chin, 2018).

Equation 2.1 below, based on Lyngfelt (1981), shows the relation of all previously mentioned parameters which together form the conventional RM formula. The dimensioning flow (Q_d) is calculated as the rainfall intensity (i) over the return period and concentration time, multiplied with the total catchment area (A_t) and the runoff coefficient (φ), which together express the reduced area participating in the runoff ($A_t \cdot \varphi$) (SV, 2016). Table 2.1 presents some established tabulated values that can be used as runoff coefficients for catchment areas with mixed land types (SV, 2016; Lyngfelt, 1981). Furthermore, the rain duration (t_r) is assumed to be equal to the concentration times (t_c), as mentioned above. This is only valid for $t_c > 10$ minutes, otherwise t_c should be assumed to 10 minutes (SV, 2016; Lyngfelt, 1981).

$$
\begin{gathered}
Q_d(T) = i(t_r, T) \cdot A_t \cdot \varphi \\
t_r = t_c
\end{gathered}
\tag{2.1}
$$

$Q_d(T)$	Dimensioning flow	(l/s)
T	Rain return interval	$(months)$
$i(t_r, T)$	Rain intensity	$(l/s \cdot ha)$
t_r	Rain duration	(min)
φ	Runoff coefficient	$(-)$
A_t	Catchment area	(ha)
t_c	Concentration time	(min)

Table 2.1: *Runoff coefficients for different land types (SV, 2016; Lyngfelt, 1981).*

Area	**Runoff coefficient** $(-)$
Roofs	0.9
Concrete and asphalt surfaces, exposed bedrock in heavy tilt	0.8
Stone surface with area with gravel joints	0.7
Gravel road, heavy tilted enriched park area without significant vegetation	0.4
Expose bedrock, not too steep	0.3
Gravel floor and gravel walkway, undeveloped neighbourhood land	0.2
Park with rich vegetation and hilly mountainous woodland	0.1
Agricultural land, grassland, meadows	0-0.1
Flat, densely forested land	0-0.1

Larger catchment areas often consist of a complex mixture of both developed and unused land (SV, 2016). For such areas with different land types, and where the proportion of developed land constitutes a smaller part of the total area, a division of sub-areas (A_N) can simplify the calculation of the contributing runoff from the total area. The runoff coefficient is then adjusted using Equation 2.2 with regards to the different surface properties within the total area (Lyngfelt, 1981).

$$\varphi = \frac{\varphi_1 \cdot A_1 + \varphi_2 \cdot A_2 + \cdots + \varphi_N \cdot A_N}{A_t} \tag{2.2}$$

φ	Runoff coefficient	$(-)$
φ_N	Runoff coefficient for sub-area N	$(-)$
A_N	Sub-area N	(ha)
A_t	Catchment area	(ha)

The rain intensity can be calculated by Equation 2.3 (Lyngfelt, 1981). Judging by its composition, the intensity seems to only depend on the rain duration in this equation, but the return period is considered by the coefficients a, b and c. These coefficients consist of empirical values, determined for different return periods and geographical locations. Table 2.2 presents the corresponding values evaluated for Gothenburg according to Lyngfelt (1981).

$$\begin{aligned} i(t_r) &= \frac{a}{t_r + b} + c \\ t_r &= t_c \end{aligned} \tag{2.3}$$

i	Rain intensity	$(l/s \cdot ha)$
t_r	Rain duration	(min)
t_c	Concentration time	(min)
a, b, c	Coefficients	$(-)$

Table 2.2: *Values for coefficients a, b and c for Gothenburg and different return periods, according to Lyngfelt (1981).*

Return period $(years)$	**a**	**b**	**c**
5	3 950	12	6
2	2 790	10	6
1	2 000	9	6
1/2	1 430	8	6
1/3	1 130	7	6

To calculate the concentration time within the catchment area, the runoff time at the land surface (t_{land}) and from diversion (t_{div}), such as via ditches or pipes, are summarized according to Equation 2.4, based on SV (2016). The concentration time is thus described as the sum of the ratios between the longest runoff distance (L_{land}, L_{div}) and the flow velocity (v_{land}, v_{div}) for both land and diversion. A correction factor of 60 s/min is also added to the ratios for correct unit conversion.

$$t_c = t_{land} + t_{div} = \frac{L_{land}}{v_{land} \cdot 60} + \frac{L_{div}}{v_{div} \cdot 60} \tag{2.4}$$

t_c	Concentration time	(min)
t_{land}	Runoff time on land surface	(min)
t_{div}	Runoff time for diversion	(min)
L_{land}	Longest runoff distance on land surface	(m)
v_{land}	Flow velocity on land surface	(m/s)
L_{div}	Longest runoff distance in diversion	(m)
v_{div}	Flow velocity in diversion	(m/s)

Table 2.3: *Water velocity in different types of diversion, according to Lyngfelt (1981).*

Type of diversion	**Velocity** (m/s)
Ordinary pipe	1.5
Tunnel and greater pipe	1.0
Dike and gutter	0.5
Soil	0.1

2.1.2 Svenskt Vatten

The report P110 - Drainage of storm-, drainage- and wastewater (SV, 2016), is a manual published by Svenskt Vatten (SV) for the purpose of ease the dimensioning of drainage systems. During the dimensioning of stormwater systems, P110 utilizes a refined version of the RM, which will be further described in this section (SV, 2016).

One of the main differences between the RM and the SV's version of RM described in P110 (SV-RM) is that a climate factor (cf) is added in the approximation of the dimensioning flow (Q_d) in the latter one (SV, 2016). The calculation of the rain intensity (i) also differs and is described as a general formula in P110 adapted to fit rain intensities around the globe. Otherwise, the relationship between duration and return period is still the same as in the conventional RM, where the intensity can be obtained from IDF plots and selected as a constant value for a certain return period and a duration corresponding to the concentration time.

To enable designs of stormwater systems that are adapted to future changes in precipitation, a climate factor (cf) is added as previously mentioned (SV, 2016). It is dependent on geographical location and rainfall duration, and is also greatly influenced by the assessments made of the climate scenarios (RCP) for global future greenhouse emissions. Based on the state of knowledge at 2015, a set of general climate factors for Sweden presented below in Table 2.4 and 2.5 have been assessed by SMHI (2015b). Table 2.4 accounts for which factors are recommended for rainfall durations shorter than one hour and up to one day, while a future percentage increase of the climate factors for a 10-year rainfall is reported in Table 2.5 for different climate scenarios (RCP mean and high).

Table 2.4: *General climate factors in Sweden, depending on rain duration (SMHI, 2015b; SV, 2016).*

Rain duration (h)	**Climate Factor** ($-$)
<1	>1.25
<24	>1.20

Table 2.5: *Percentual increases of climate factors for different rain durations of a 10 year rain, for both the mean and the high RCP climate scenarios (SMHI, 2015b). The latter scenario is the most conservative, pessimistic option among the simulations by SMHI (SMHI, 2015b; SV, 2016).*

Rain duration (h)	**2021-2050** ($-$)		**2069-2098** ($-$)	
	Mean	**High**	**Mean**	**High**
0.3	1.19	1.23	1.30	1.51
1	1.14	1.16	1.20	1.34
3	1.13	1.13	1.17	1.29
12	1.12	1.14	1.18	1.29

The catchment area and the rain duration are estimated equally as described in Section 2.1.1, where the runoff coefficients (φ) remain the same as in Table 2.1 and the rain duration (t_r) is equal to the concentration time (t_c). In total, the dimensioning flow is calculated according to Equation 2.5 (SV, 2016). If the runoff coefficient needs to be altered according to different land covers in the catchment area, the Equation 2.2 in Section 2.1.1 could be utilized.

$$\begin{gathered} Q_d = i(t_r, T) \cdot A_t \cdot \varphi \cdot cf \\ t_r = t_c \end{gathered} \tag{2.5}$$

Q_d	Dimensioning flow	(l/s)
$i(t_r, T)$	Rain intensity	$(l/s \cdot ha)$
t_r	Rain duration	(min)
t_c	Concentration time	(min)
A_t	Catchment area	(ha)
φ	Runoff coefficient	$(-)$
cf	Climate factor	$(-)$

The concentration time (t_c) is calculated in the same fashion as in Section 2.1.1 and Equation 2.4. To calculate the runoff time from the catchment area and the diversion, either tabulated values could account for the velocity, or it could be calculated. Tabulated values are listed in Table 2.3. According to SV (2016), the velocity of the runoff should be calculated by Equation 2.6 if the type of diversion is soil. The Manning's coefficients for regular land types and diversions are found in Table 2.6 (SV, 2016). The Equation 2.6 can also be used to calculate the velocity for water in canals (Bondelind and Häggström, 2018). In this case, the R represents the Hydraulic radius and is calculated as a ratio between the wet cross section (A_p) and the wet perimeter (P) (Bondelind and Häggström, 2018; SV, 2016). The relation between the wet cross section's area and the wet perimeter is illustrated in Figure 2.2.

$$\begin{gathered} v = M \cdot \sqrt[3]{R^2} \cdot \sqrt{S} \\ R = \frac{A_p}{P} \end{gathered} \tag{2.6}$$

v	Velocity of runoff water	(m/s)
M	Manning's coefficient	$(\sqrt[3]{m}/s)$
R	Water depth or hydraulic radius	(m)
A_p	Wet cross section's area	(m^2)
P	Wet perimeter	(m)
S	Gradient of area or creek bed tilt	(m/m)

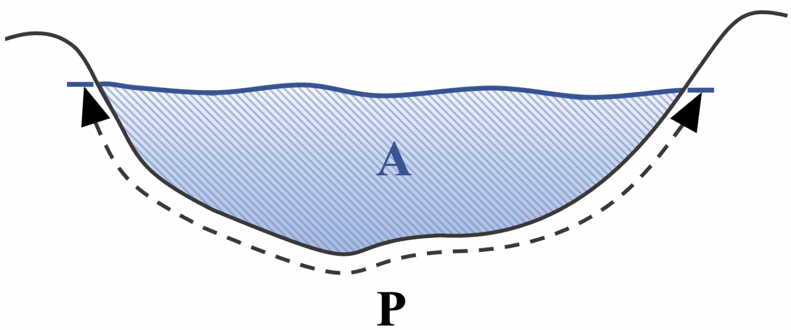

Figure 2.2: *Illustration of a canal's wet cross-sectional area and wet perimeter. Authors own figure, inspired by Bondelind and Häggström (2018).*

Table 2.6: *Manning's coefficient for different type of runoff sections, modified table from (SV, 2016).*

Runoff type	Specified	Manning's coefficient ($\sqrt[3]{m}/s$)	
		Natural	**Constructed**
Land	Busch field	5	
	Grass field	20	
Canals/Creeks/Ditches	Much vegetation	10	10
	Some vegetation	25	30
	No vegetation	30	50
Coated Canals	Coarse concrete		50
	Fine concrete		65
	Wood		65

The rain intensity is calculated by Dahlström's Formula according to Equation 2.7, which is adjusted to Swedish conditions (Dahlström, 2010). The formula is highly dependent on the return period (T) and the concentration time (t_c) (Dahlström, 2010; SV, 2016; STA, 2017). Additionally, it is valid for return periods between 1 month up to 10 years and during concentration times that vary between 5 minutes to 24 hours (STA, 2017; Dahlström, 2010).

$$i(t_c, T) = 190 \cdot \sqrt[3]{T} \cdot \frac{ln(t_c)}{t_c^{0.98}} + 2 \tag{2.7}$$

$i(t_c, T)$	Rain intensity	$(l/(s \cdot ha))$
T	Rain return interval	$(months)$
t_c	Concentration time	(min)

In P110 (SV, 2016), the importance of assessing the impact of natural land runoff is underlined when using the RM for estimates of more or less undeveloped areas. The assessment of the runoff time for the total catchment area is further stated as the difficult part, but that a low value of the runoff coefficient for the natural land is often used for consideration of its impact. Furthermore, it is also stated that estimation methods can be used to estimate dimensioning flows from natural land, for example by using a diagram that shows the specific flow as a function of size (in hectares) for an average catchment area and for different return times (5 -100 years). The data that the diagram is based upon is described to originate from observations of runoff from precipitation-rich areas in western Sweden, consisting of average forested/agricultural land.

2.1.3 The Swedish Transport Administration

In 2010, the Swedish Transport Administration (STA) inherited calculation methods for dimensioning of infrastructure from the Swedish Road Administration, and since then many alterations have been refined. These methods are compiled in a document with advises that STA use as guidelines, referred to as TRVINFRA (STA, 2021a), which within time will replace the previous version entitled as MB310 (STA, 2017). At the time of writing this thesis, both documents are valid, since MB310 is still used in projects initiated before 2020 when TRVINFRA got introduced.

To calculate the dimensioning flow from a catchment area, the guiding documents advises another version of the RM as well as methods according to P110 (SV, 2016). The version is adapted with considerations to the infiltration and potential storage capacity of permeable surfaces, due to their great potential pore volume. The abundance of rainwater runoff that is not infiltrated or stored is to be considered as the dimensioning flow, which is calculated at either an outlet point or a connection point of the runoff infrastructure. On an annual basis, flows also need to be calculated with regard to different rain intensities and durations, as the annual precipitation varies over the year (STA, 2021a).

TRV INFRA also clearly states that the version of RM only should be utilized in road near areas in which the majority of the runoff originates from the road surface. In cases in which the natural land is predominant, TRV Infra the method of Natural land runoff described in P110 *should* be utilized, although SV (2016) themselves only state the method *could* be used.

The calculations according to the RM version is applied as follows; The rain intensity (i) is calculated by Dahlström's formula which is the same formula as mentioned in Section 2.1.2. For some Swedish cities, statistics of precipitation rate and intensity are available and can be used for more accurate predictions. Generally, the formula is considered valid for return periods (T) ranging between 1 month up to 10 years and during concentration times (t_c) that vary between 5 minutes to 24 hours. However, both documents implies that the formula should be used for return periods up to 20 years, but STA (2021a) also claims it to be acceptable for return periods up to 100 years. Furthermore, the t_c is calculated as described in Section 4.5 and Equation 2.4 but with velocities described in Table 2.7 (STA, 2021a). The dimensioning rain return period is predetermined due to the expected consequences when the capacity is exceeded. During rainfalls with short duration, the flat surfaces are expected to possess a storage capacity that is capable of managing a high rain intensity. If the runoff in the area has an expected concentration time longer than 15 minutes, that computed time should be selected. The concentration time is also calculated in the same fashion as described in Section 2.1.2.

Table 2.7: *Water velocity in different types of diversion (STA, 2021a).*

Type of diversion	**Velocity** (m/s)
Ordinary pipe	1.5
Tunnel and greater pipe	1.0
Dike (often carrying water) and gutter	0.5
Dike (rarely water carrying) and gutter	0.2
Soil	0.1

As can be seen in Tables 2.8 and 2.9 below, only runoff coefficients for impervious surfaces (φ_{imp}) are advised, for different rain intensities (i) according to STA (2021a) and in general according to STA (2017). The reason why the tables does not present any permeable surfaces is simply since Equation 2.8 does not consider any runoff coefficient for permeable surfaces. Instead, a factor describing the infiltration capacity (f_i) is utilized for the permeable surfaces in the road near areas.

Table 2.8: *Runoff coefficients for different land covers and rain intensities* $(l/(s \cdot ha))$ *(STA, 2021a).*

Land cover	**Runoff coefficient** $(-)$		
	i = 15	**80 > i > 100**	**i > 200**
Coated road surface	0.7	0.9	0.95
Uncoated road surface	0.6	0.8	0.87
Other types of hardened surfaces	≤ 0.7	0.6-0.9	0.73-0.95

Table 2.9: *Runoff coefficients for different land covers (STA, 2017).*

Land cover	**Runoff coefficient** $(-)$
Coated road surface	0.9
Uncoated road surface	0.8
Other types of hardened surfaces	0.6-0.9

Further, STA (2021a) advises to multiply the dimensioning flow by a climate factor (see Table 2.10), with the notation that a climate factor for 1.2 is sufficient for the most cases of natural land runoff. It is then described that the worst cases at 100-year flows must also be multiplied by a factor of 2.4 (STA, 2021a).

Table 2.10: *Climate factor for different rain durations (STA, 2021a).*

Rain duration (h)	**Climate factor** $(-)$
≤ 1	1.3
1-24	1.2

Generally, road areas and banks are designed with an adequate permeability (STA, 2017). Values of the infiltration capacity (f_i) can be assumed according to Table 2.11. However, this capacity can be higher, but greater values could only be appointed after verification tests have been conducted in the field.

Table 2.11: *Infiltration capacity for land covers (STA, 2017).*

Type of permeable surface	**Infiltration capacity** $(l/(s \cdot ha))$
Vegetation-covered areas within the road area	>100
Grassy slopes and ditches	>150

The dimensioning flow is calculated according to Equation 2.8 (STA, 2017). The rain intensity is calculated by the same formula as stated in Section 2.1.2 and Equation 2.7.

$$Q_d = i(t_c, T) \cdot A_{imp} \cdot \varphi_{imp} + A_p \cdot (i(t_r, T) - f_i) \tag{2.8}$$

Q_d	Dimensioning flow	(l/s)
$i(t_c, T)$	Rain intensity	$(l/s \cdot ha)$
T	Return period	$(months)$
A_{imp}	Impervious area	(ha)
φ_{imp}	Impervious runoff coefficient	$(-)$
A_p	Permeable area	(ha)
f_i	Infiltration capacity	$(l/s \cdot ha)$

According to STA (2021a), the design of culvert pipes is also restricted under certain advices including elevation and slope. The design and elevation setting of a pipe with a circular cross-section should be established so that the water level at the dimensioning flow event does not exceed 85% of its dimension. In addition, as shown in Figure 2.3, culvert pipes must be dimensioned with a so-called shallow depth which means that their lower inner edge is lowered in relation to the bottom level of the connecting watercourse or ditch. This promotes the hydraulic properties of the culvert pipe and reduces the risk of under-flushing as it becomes more difficult for water to divert on the outside of the pipe. Since bottom material in the form of stone and gravel is transported by watercourses, the shallow depth will to some extent get filled with material that creates similar conditions as in the natural watercourse bed. However, for pipes with a large shallow depth and long span, the bottom material may need to be filled beforehand at installation to create such favourable conditions. The filling material must for these cases be adapted so that they resemble the natural bottom substrates, specially for pipes that functions as aquatic fauna passages.

Furthermore, culvert pipes intended for aquatic fauna passages should be constructed with a slope between 0-5 ‰ adapted based on the slope of the watercourse, which is decisive (STA, 2021a). A slope greater than the specified range can be accepted as long as the structure maintains an acceptable function for the aquatic fauna passage. The structure must also be designed to withstand certain high flows without exceeding the velocity of the watercourse inside the pipes. These flows, called *Mean high flows* (MHQ), are not directly connected to a rain scenario but are predicted with a return period of 1-2 years.

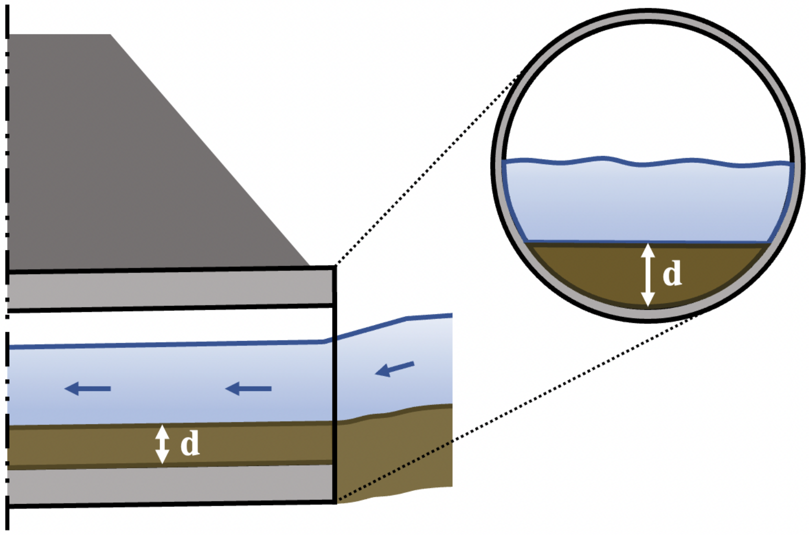

Figure 2.3: *Illustration of the shallow depth, denoted as d, in a culvert pipe for aquatic fauna passage. Authors own figure, inspired by STA (2017).*

2.1.4 Time-area method

According to SV (2016), the Time-area method (T-A) is described as a graphical approach that enables flow calculation considering different runoff times for different participating areas within a catchment area. Due to spatial differences in rainfall duration and intensity, varying runoff times in different areas can thus be taken into account. This makes T-A particularly suitable for peak flow calculations within larger catchment areas, referred to areas larger than 20-30 ha.

The approach includes the production of so-called isochrons, lines that describe and link specific runoff times from different reduced areas to a specific calculation point SV (2016). When plotted in a Time-Area Histogram (TAH), the isochrones function as a linear relation between reduced contributing area and longest runoff time. A breaking point of this relation occur when the total reduced area is reached for the longest runoff time within a sub-area, after which the reduced area remains constant with time. This is illustrated in Figure 2.4a, where the coloured lines correspond to the isochrones of the different sub-areas illustrated in Figure 2.5. The black line presents the total runoff for the total catchment area, i.e. the summation of all individual isochrones, often referred to as the TAH (Sabzevari, 2017). Figure 2.4b further shows a parallel shifting of the TAH where it is replicated at regular intervals corresponding to the duration of the rain until the first sub-catchment area starts to contribute to the runoff. This is useful, for example, to be able to determine the maximum reduced area at a certain rain duration even if the rain has ceased before the runoff reaches the calculation point.

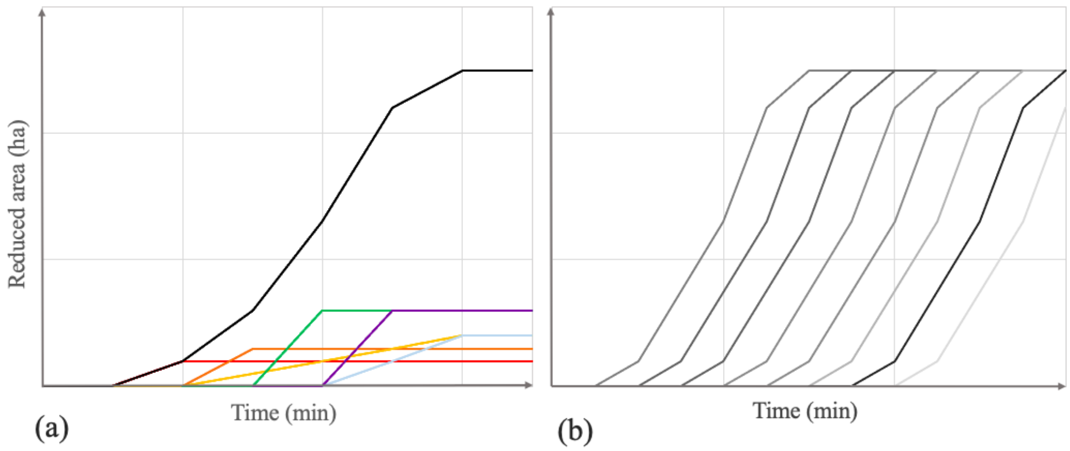

Figure 2.4: *Illustration of isochrones and the total runoff's Time-Area Histogram (TAH) in (a), and of the TAH with replicates shifted in parallel in (b). Both based on the sub-catchment areas in Figure 2.5. Author's own figure, inspired by SV (2016).*

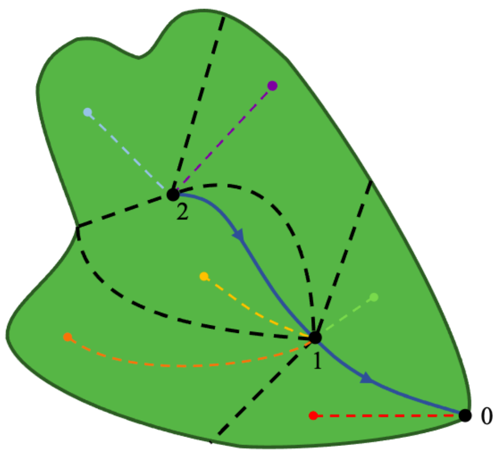

Figure 2.5: *Schematic illustration of a catchment area divided into the different sub-areas plotted in Figure 2.4. Black dashed lines present the sub-catchment borders, coloured presents the longest runoff distance within each sub-catchment area. The connection points to the main line, for this case in a creek, are marked with black dots. The longest runoff distance for each sub-area is thus the coloured dashed line plus the eventual travel distance in the creek. Author's own figure, inspired by SV (2016).*

In short, the T-A method overall means that a catchment area first is divided into different sub-areas (see Figure 2.5), where the runoff within each area is represented by a specific time and flow, which can be calculated with the RM (SV, 2016). The additional runoff that remains from the outlet point of each sub-area to the determined calculation point for the total catchment area, is the one described by the isochrones, which depicts the different contributing areas at different rain durations. By first sum up all isochrones and shifting the total TAH as described above, the total runoff in the catchment area can then be calculated by multiplying the maximum reduced area by the rain intensity specific to the duration and return period of the studied rain event.

2.1.5 Flödesappen

Flödesappen is a web-based program that the STA currently are developing together with the executing consulting firm *Geografiska informationsbyrån (eng. Geographical Information Bureau)*. The idea behind the application was developed as a response to the increased stormwater flows due to climate change, with the aim of promoting the work of assessing risks that this may entail against socially important operations at critical points, such as infrastructure networks and installations at low points (Lindeberg et al., 2019). Additionally, the goal is for the application to become a simple tool that estimates dimensioning water flows by performing calculations of upstream catchment areas. The user interface of the app is shown in Figure 2.6 below.

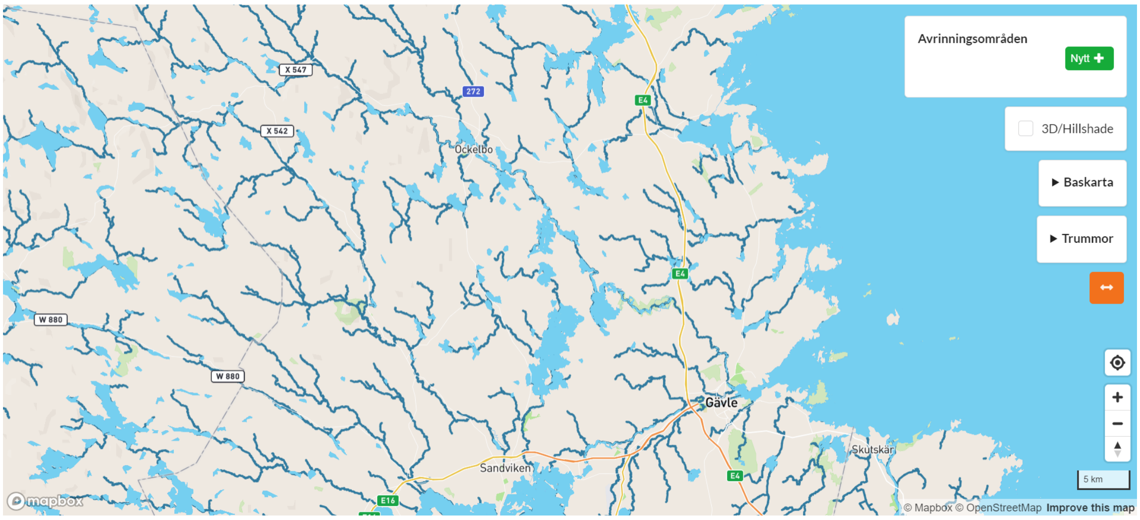

Figure 2.6: *An example of the general user interface of Flödesappen. Screenshot taken from the website of the app (STA, nda).*

As a basis for calculating catchment areas, the app uses a processed elevation model with a raster grid of flow directions where the water can flow in eight different directions at each grid point Lindeberg et al. (2019). The sidebar menu on the right side in the interface, as shown in Figure 2.6, provides some different user opportunities, for example to select different map layers as background under the field *"Baskarta"*. The main function is, however, applied by clicking on the green button in the field

"Avrinningsområde". This allows the user to place a pin at any hydrograph-line on the map to obtain the calculated catchment area and its dimensioning flow for that specific point, as can be seen in Figure 2.7. The data for all points on the map have thus already been calculated and stored in order to be able to quickly give a result. For example, as shown in the results window on the left in Figure 2.7, the exemplified catchment area have a total area of 9.27 km^2, with a share of 0.04 % corresponding to lake surface area, and a longest runoff distance estimated to 8 069 m. Results of the different shares of land covers in the catchment area can also be retrieved under the field *"Marktäcke"*.

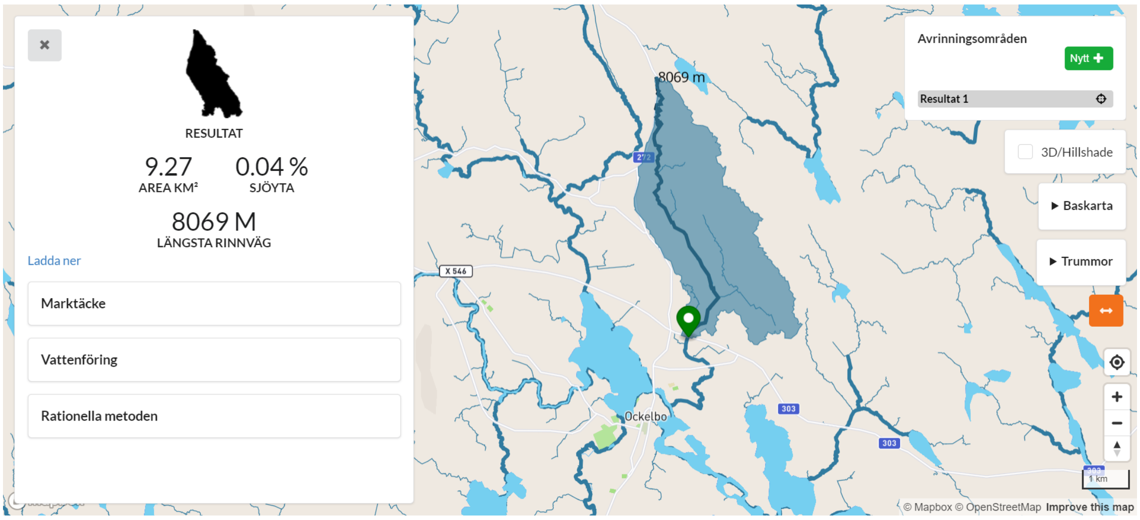

Figure 2.7: *The user interface of the first overview of an exemplified result in the Flödesappen. Screenshot taken from the website of the app (STA, nda).*

The app is based on two different, main empirical methods for calculating dimensioning water flows, which in turn are based on different assumptions and input data. The first one is reached under the middle field *"Vattenföring"* in the result window to the left as shown in Figure 2.7. This calculation form includes data from measurements of catchment areas with known properties and can be described as a flow statistic method. By that, flows for different return periods, calculated on the basis of two different intervals of statistical annual data and for different climatic factors, can be obtained. The calculation can also be applied so that the result is based on MB310 and/or TRVInfra.

Furthermore, the second calculation method is the RM which is applied as a separate feature within the app, under the field *"Rationella metoden"* as also can be seen in the result window in Figure 2.7. This RM application is defined with an areal limit which in turn is specified so that the catchment areas have to be less than 100 ha to make the feature applicable. The calculations of the flow and rain intensity are based on the same equations as mentioned earlier in Section 2.1.2, see Equations 2.5 and 2.7. However, the main difference is that different runoff coefficients, shown in Table 2.12 below, are assumed for Flödesappen compared to the ones used in the SV-RM calculation process (see Table 2.1).

Table 2.12: *Runoff coefficients for different land covers (Lindeberg, 2020).*

Land cover	**Runoff coefficient** $(-)$
Exploited land, buildings	0.9
Exploited land, roads	0.8
Exploited land, excluding roads and buildings	0.7
Unvegetated open field	0.3
Unvegetated wetland	0.2
River and creeks	0.2
Agricultural land	0.1
Clear felled area	0.15
Vegetated open field	0.05
Forest in and out of wetland	0.05
Water bodies	0

It is important to highlight that the application is under developing progress. At the time of writing this thesis, there are thus some limitations that have not yet been dealt with. For example, not all roads have been “cut” at the locations of existing culvert pipes, meaning that water accumulates at the road instead of being transported through the culvert pipes as in real life. The road thus becomes a basin at these locations. However, a temporary solution to this meanwhile is that when the hydrographic lines meet an elevated obstacle in the terrain that is less than a certain length (round 15 meters), such as a road bank, it breaks through anyway (A. Gunnarsson, personal communication, 20th of May 2022).

Another current limitation in the app is that generated catchment areas can not be divided or merged. This is mentioned in the development report by Lindeberg et al. (2019) as an improvement point that would give the user the opportunity for extended flow calculations. It is also mentioned as a solution to overcome some deviations related to the accuracy of the elevation model, for example get around changes in the landscape originating from anthropogenic activities.

2.2 Dimensioning with Colebrook’s method

A method that is commonly utilized for the dimensioning culvert pipes and regular pipes is the Colebrook’s method, sometimes referred to as the Colebrook-White Equation (Brkić, 2011). The method was first introduced in 1934 as an equation, which later have been developed into diagrams, for convenience (Brkić, 2011). Oftentimes, the Rational Method (RM) utilizes its calculated flow to decide upon which size of culvert pipe that is necessary to facilitate that particular flow.

The diagram is available for a range of roughnesses, which refers to the smoothness of the of the water-bearing surface. Where a rough surface like concrete has a greater value, and a fine surface like plastic a lower (SLU, 2014). Figure 2.8 presents the Colebrook’s diagram for roughness 1.0 mm. In Appendix A, the diagram for

0.2 mm is also presented. To be able to use the diagram, two out of three parameters need to be known; water velocity, water flow or pipe gradient (SV, 2016). The water velocity can be determined either by calculations or eventual regulations (in pipelines etc.), whereas the flow is determined by Equation 2.1, 2.5 or 2.8. Regarding the pipe gradient, regulations may determine arbitrary values depending on the type and function of the infrastructure (STA, 2017, 2021a). The known parameters will give a value that lies between two dimensioning lines in the diagram, where the larger pipe dimension should be chosen since the dimension always should be conservatively selected to avoid underestimation.

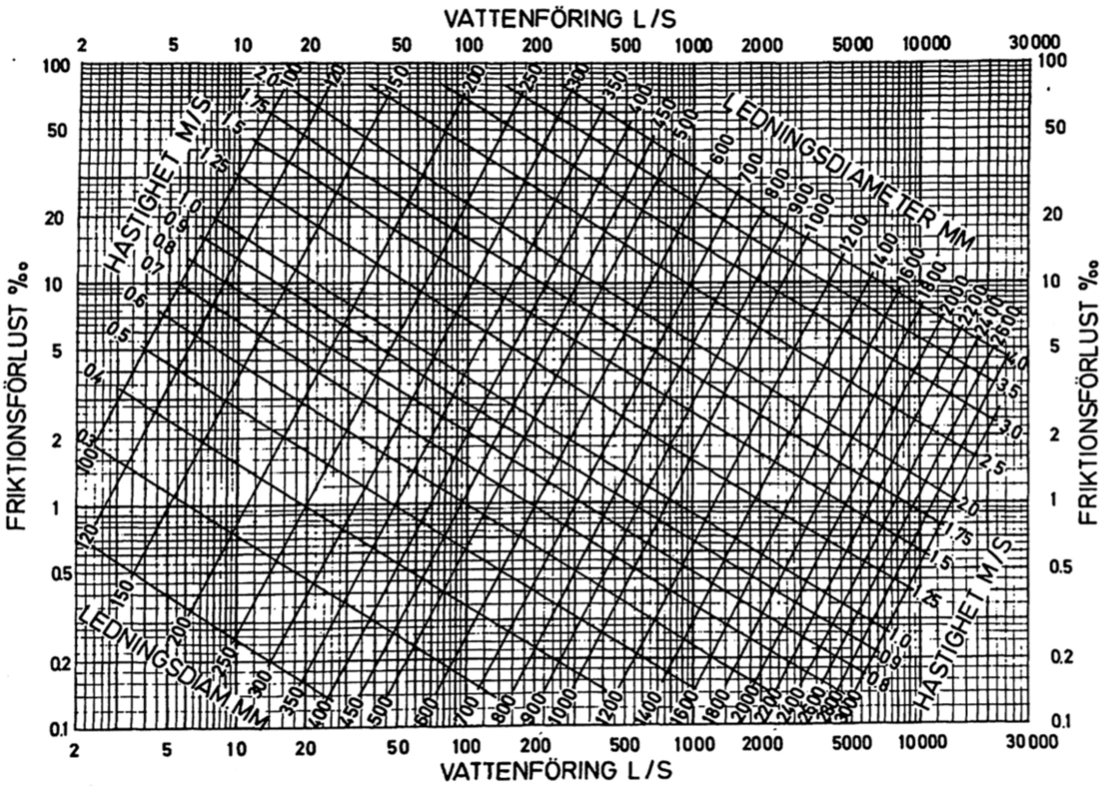

Figure 2.8: *Colebrook's diagram for rawness k = 1.0 (mm) (SV, 2016). Translation: "Vattenföring L/S" = Flow (l/s), "Friktionsförlust ‰" = Pipe gradient (‰), "Ledningsdiameter MM" = Pipe dimension (mm) and "Hastighet M/S" = Water velocity (m/s).*

The pipe material determines which roughness the method entails. Roughnesses for typical culvert pipe materials are stated in Table 2.13 (SLU, 2014). However, the STA (2021a) advises that the roughness factor always should be assumed to 1.0 mm when utilizing the Colebrook's method, regardless of culvert pipe material.

Table 2.13: *Roughness coefficient for different culvert pipe materials (SLU, 2014).*

Culvert material	**Concrete**	**Steel**	**Plastic**
k (mm)	1.0	0.5	0.05

The dimensioning process of culvert pipes according to SV (2016) states that the degree of filling for a culvert pipe should not be 1:1. As mentioned in Section 2.1.3, TRVINFRA also indicates flow limit to 85 % of the full pipe dimension. (STA, 2021a). Before employing the Colebrook's diagrams, P110 therefore considers a degree of filling in the culvert pipes. This degree can be presented as a maximum flow percentage describing the maximum permissible fullness of the culvert pipe (X), in turn defined as the quota between the culvert pipe flow when completely filled (Q_{full}) and the flow for the desired culvert pipe dimension ($Q_{d,new}$). It can also be described as a ratio between the maximum filling height (y) and pipe dimension (D).

If the degree of filling is described as a maximum flow percentage of the full culvert pipe, the new dimensioning flow ($Q_{d,new}$) is calculated as in Equation 2.9.

$$\begin{aligned} X &= \frac{Q_{full}}{Q_{d,new}} \\ Q_d &= Q_{full} \end{aligned} \tag{2.9}$$

X	Maximum fill flow	(%)
Q_{full}	Flow for filled culvert pipe	(l/s)
Q_d	Dimensioning flow	(l/s)
$Q_{d,new}$	New dimensioning flow	(l/s)

If the maximum filling instead is described in maximal filling height in relation to the pipe dimension, this relation is described in Equation 2.10 (SV, 2016) and Figure 2.9.

$$\frac{Q_{full}}{Q_{d,new}} = 0.46 - 0.5 \cdot cos\Big(\frac{\pi \cdot y}{D}\Big) + 0.04 \cdot cos\Big(\frac{2 \cdot \pi \cdot y}{D}\Big) \tag{2.10}$$

$Q_{d,new}$	New dimensioning flow	(l/s)
Q_{full}	Flow for filled culvert pipe	(l/s)
y	Filling height	(m)
D	Culvert pipe dimension	(m)

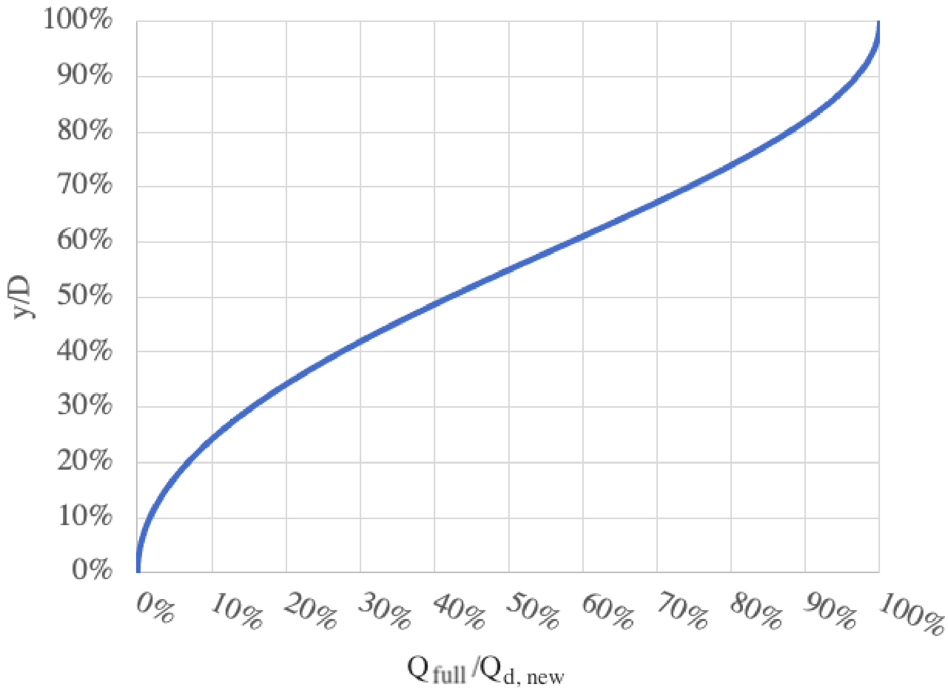

Figure 2.9: *The partial fill diagram of a culvert pipe, Authors' own figure, based on Equation 2.10 (SV, 2016).*

Figure 2.9 translates the relation between the filling height and the culvert pipe dimension to the degree of filling of the pipe, which then can be put into Equation 2.9 to calculate the new dimensioning flow. The figure is based on Equation 2.10.

2.3 Weather data

Since many of the running weather measuring stations nowadays only have been collecting data since the 1960's or shorter, some weather predictions can be conceded unreliable. A few methods have been developed to get around this issue, and one of those is the Station-year method (SMHI, 2017). This method is further described in Subsection 2.3.1, followed by Subsection 2.3.2 which covers techniques of collecting and measuring precipitation data.

2.3.1 Station-year method

The Station-year method combines data from several measuring stations in the vicinity of the area in question (SMHI, 2017). The method assumes that the different stations are not related, and are to be considered as independent (SMHI, 2021a). Therefore, much larger amounts of independent data can be considered and put into an extended time series, to thereby determine rain with larger return periods (SMHI, 2017). The sources of error with this method includes, among others, that the results could be biased if the stations are too close to each other (SMHI, 2021a).

The Swedish Meteorological and Hydrological Institute (SMHI) divided Sweden into four regions for extreme and short term (less than 12 hours) precipitation: northern (N), central (M), as well as southwest (SW) and southeast (SE) (SMHI, 2017). The division could help to sort precipitation data in the order of magnitude and reach a solid foundation for statistics for each region.

2.3.2 Measurement of precipitation

In the traffic infrastructure industry, there are two main distributors of weather data that collect the most information from weather data in Sweden; the STA or SMHI. These authorities use different collection and measurement systems which are further described in the following Subsections 2.3.2.1 and 2.3.2.2.

2.3.2.1 VViS

In order to enable prediction and prevention of slippage and black ice, the STA has installed own road weather stations (VViS) in places along prioritized state roads in Sweden where the risk of icy roads is judged to be greatest (STA, ndc). The system was developed to help the winter road maintenance staff to *"perform the right actions at the right time"*, and it has been used by The STA to collect weather data since the 1980's (STA, 2016). In addition to increasing safety and accessibility on roads through more efficient winter road maintenance, VViS is also an important part of reducing both environmental impact and costs related to winter road maintenance, such as by adapting and regulating road salt use (Jonsson, 2019).

In 2019, the number of existing VViS stations amounted to 775, each with the capacity to measure various weather parameters including temperature, humidity and type and amount of precipitation (STA, ndb). These measuring stations (MS4), developed during the late 20th century, are in their final phase of usability and have therefore begun to be replaced with new measuring stations (MS7) with modern technology and higher performance sensors (Jonsson, 2019). The installation of the new sensors began during the winter season 2019-2020 by gradually establishing MS7 stations in parallel with some already existing MS4 to compare and evaluate their performance (Jonsson, 2020). Through this, many similarities have been distinguished between the measurement results for the two different sensors, but also several differences. The study for example indicates increasing deviations in precipitation between MS4 and MS7 under windy weather conditions, and that MS4 in some cases with either stronger winds or intense snowfall has underestimated the precipitation of snow. Furthermore, the MS7 sensor (PWD22) has a measurement accuracy of $\pm 10\%$ to $\pm 15\%$, in comparison to $+15\%$ to $+30\%$ for the MS4 sensor (Optic-Eye) (Vaisala, 2018; ASFT Industry AB, nd).

2.3.2.2 Geonor

SMHI has been collecting weather data in Sweden since the 1960's, and in 2006, the authority had over 120 measuring stations in operation (Dahlström, 2006). Since 1995, the majority of the weather stations have been redone according to international standards and certifications (SMHI, 2017).

At least once an hour, the measuring system collects data for each weather station (Dahlström, 2006). The systems are fitted with a range of different weather measuring equipments, among them, a precipitation gauge from Geonor (accuracy 0.1%, FS 0.6mm). Dahlström (2006) mentions some uncertainties of the Geonor precipitation measurements including, for example, the wind moving water particles from the collection container or if the precipitation fall as snow. When the snow melts in the warm container, vaporization may then occur. However, as the measurement method is based on the weighting of precipitation, it is therefore considered to be accurate at high intensities (Dahlström, 2006).

3
Case study

As can be seen in Figure 3.1, the investigated case studies are located in Gävleborg county (see (a)), north of Gävle in an urban area called Ockelbo (see (b)). More in particular, Case 1 consists of a culvert pipe southwest of Ockelbo, while the culvert pipe in Case 2 is found northwest of the urban area (see (c)).

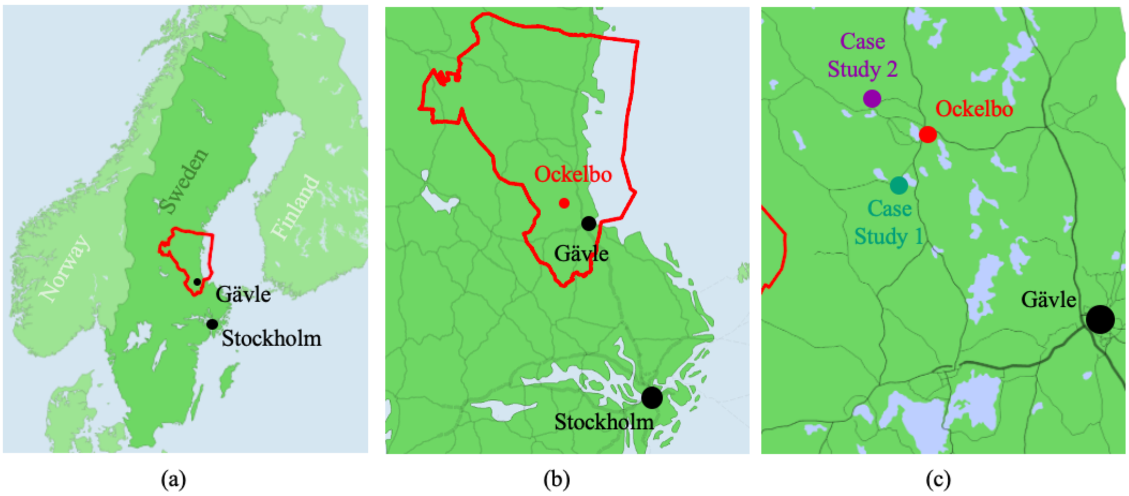

Figure 3.1: *A map of the case studies' areas. The background maps collected from the National Swedish Land Survey (nd).*

In August 2021, Gävleborg was one of the counties suffering the most by the extreme rainfall that fell over the central parts of Sweden (MSB, 2021). It was on the late afternoon to night between August 17th and 18th that the rainstorm hit. Within a week later, the extreme event had broken several records, including the highest rainfall ever measured by the Swedish Meteorological and Hydrological Institute (SMHI) for a two hour rain duration (SMHI, 2021c; SVT, 2021). This chapter further describes the studied case areas and the given data that have been utilized as background information for the performed analyses and calculations of the flows generated by this extreme rain event.

3.1 Case study 1 - Brattfors

The first case study is a culvert pipe located on the road 545 near by the village of Brattfors and the lake Hammarsjön, just south of Ocklebo. The annual daily traffic (ADT) was in 2018 assumed to 340 vehicles per day (STA, 2021b). In close proximity to the culvert pipe, the area is rural and surrounded of woodland, which also houses some smaller maintenance roads and a wind farm as can be seen in Figure 3.2a. This local area is generally dewatered by the creek Norrbäcken extending in the landscape, which consists of several branches including some parts that also goes by the name *Laxöringsbäcken*. Furthermore, a variation between exposed bedrock on the hillsides and lakes or creeks in the valleys is found in the surrounding landscape. Three mountain peaks that have exposed bedrock are Rippenberget, Mårtensklack and Trollberget (SGU, nd). Figure 3.2b shows that the underlying soil layers are mostly till, but three deposits of ice river sediments are also visible in close proximity, heading southeast, of the culvert pipe location (SGU, nd). Additionally, the lake Hammarsjön is situated on post glacial sediments of sand and gravel.

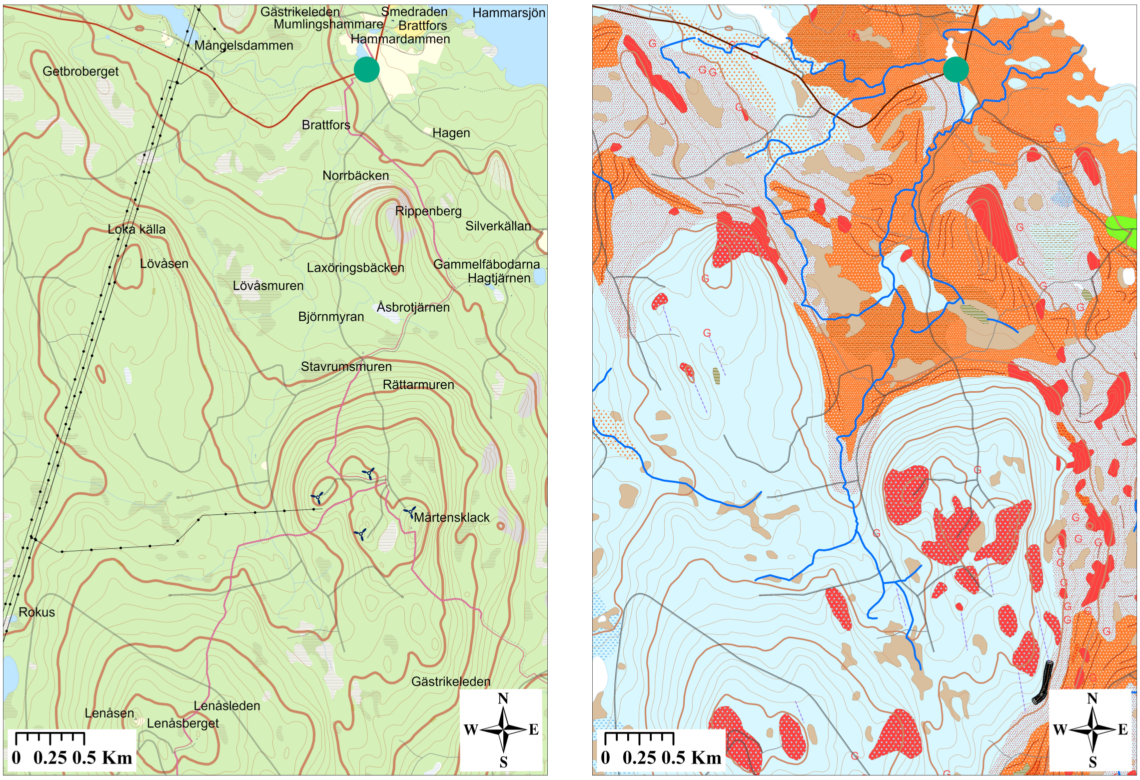

(a) **(b)**

Figure 3.2: *To the left a map of the Brattfors area. The dashed line presents a general guide of the catchment area. To the right the soil type for the same area, figure retrieved from SGU (nd).*

Sometime during the night between the 17th and 18th of August 2021, the road 545 were flushed away due to a heavy downpour, see Figure 3.3. As the figure shows, the overlying road embankment of the culvert pipe completely collapsed and created a large cavity in the road. A possible scenario that caused this collapse could be that the elevated water pressure created a force in the pipe which caused a failure in the pipe material. A crack in the pipe material could therefore have permitted a water-flow in the embankment which in turn gave rise to the collapse by eroding the bank material.

Figure 3.3: *Picture of the flushed away road embankment in Brattfors. Reprinted with permission from P4 Gävleborg/Sveriges Radio (2021).*

The culvert pipe was inventoried just over a month before the heavy rain event took place, and according to the inventory, the structure then had no obvious deficiencies. It was a circular, steel pipe with a diameter of 1600 mm and a length estimated to 11 meters. Both the functional status and material status were classified as *Åtgärd på sikt (eng. preparatory measures in time)*, which is the best marking these parameters can have. Figure 3.4a was taken in connection with this inventory. After the rain event, the construction has been refitted and now a trench-coat culvert pipe with the dimension of 1 900 mm and 20 meters dewaters the area. This new, current culvert pipe is shown in Figure 3.4b, taken by the authors during the field visit of the 28th of April 2022.

(a) **(b)**

Figure 3.4: *Pictures of the culvert pipe in Brattfors. The left one was taken before the rain incident, on July 13th 2021. The right one illustrates the new culvert pipe, inventoried during the case study visit of April 28th 2022. The STA owns the pictures.*

3.2 Case study 2 - Vallsbo

The second case study is located just north of Ockelbo, nearby the village of Vallsbo, and consist of a culvert pipe that brings the creek Norrönningsbäcken across the road 546 to the lake Vallsjön. The annual daily traffic (ADT) on the road was in 2016 assumed to 590 vehicles per day (STA, 2021b). The majority of the local area is forested, apart from some smaller maintenance roads and minor lakes or wetlands, see Figure 3.5a. In the southern parts of the area, some residences on plots of agricultural land by the lake Vallsjön are also found. Furthermore, the geology of the landscape consists of mostly till (SGU, nd) as can be seen in Figure 3.5b. However, lake Vallsjön is located in a depression of fine-grained sediments such as clay and silt, in between two stretches of glacial river sediment. Of the mountains in the area, only Yxursberget has exposed bedrock whereas Flaggberget and Gnuptjärnsmuren have not that (SGU, nd).

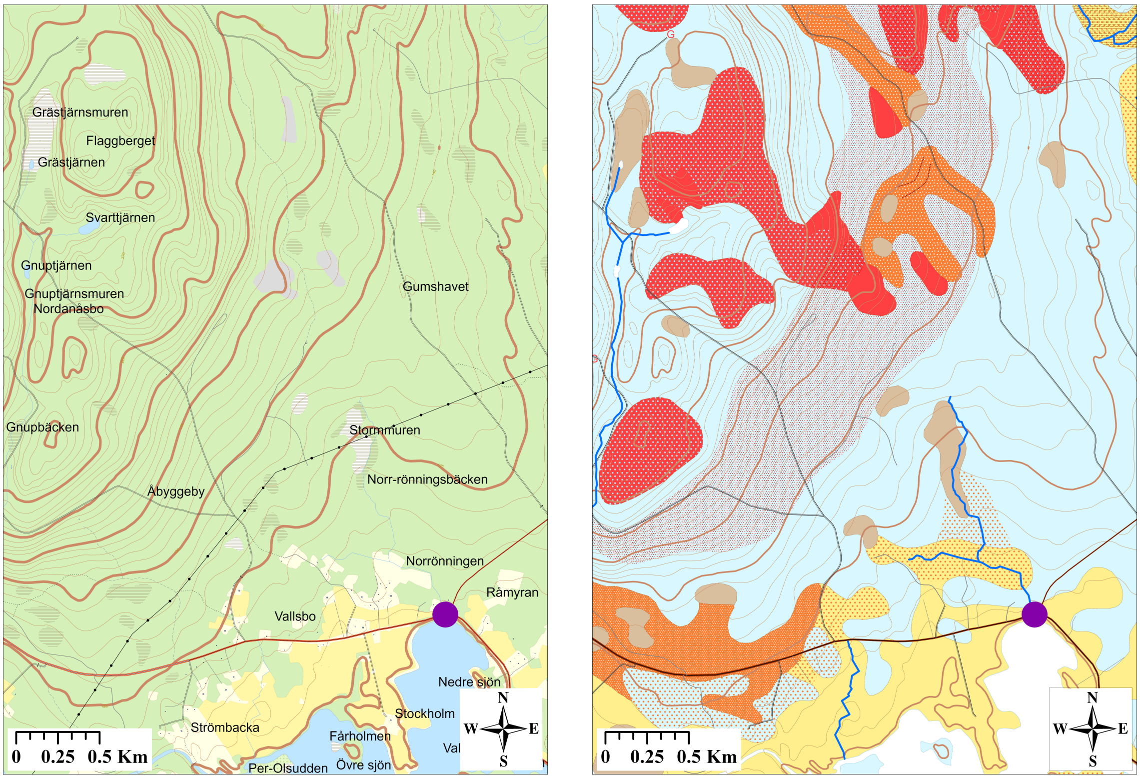

(a) (b)

Figure 3.5: *To the left a map of the Vallsbo area. The dashed line presents a general guide of the catchment area. To the right the soil type for the same area, figure retrieved from SGU (nd).*

Sometime during the night between the 17th and 18th of August 2021, the road was flooded due to a heavy precipitation. Unlike the first case study, the culvert pipe of this second study was not inventoried prior to the rain event that flooded the area. What is known about the case is therefore only what the operational managers found out during the restoration of the infrastructure. However, since the restoration, the culvert pipe has been flushed to obtain its dimensioning flow capabilities. Figure 3.6a and 3.6b below, taken by the authors during the field visit, illustrates this current culvert pipe. It has a dimension of 1 200 mm, a length of 16 meters and is made out of concrete.

(a)

(b)

Figure 3.6: *Pictures of the culvert pipe in Vallsbo, both taken after the rain incident during the case study visit of April 28th 2022. The STA owns the pictures.*

3.3 Rain event - Gävleregnet

The heavy rain of the 17th to 18th of August 2021, Gävleregnet, was powerful enough to destroy infrastructure in the Gävleborg area, and has been chosen as the dimensioning event to simulate the calculations for the two previously mentioned case studies. Data for this specific rain are available from both Geonor and VViS measuring stations. The data from VViS, STA's stations, are raw data, where each station has a precipitation measurement that is representative for a varying time period. The data from Geonor, SMHI's stations, has a convenient data retrieving format, where data can be collected per month, day or alike. Also, an analysis by SMHI (2021a) of the rain event conducted on SMHI's own measurements was available, these values are presented in Table 3.1.

Table 3.1: *The maximal measured precipitation during "Gävleregnet" at different rain duration times, and return periods calculated by the Station-year method (SMHI, 2021a).*

Rain duration (h)	**Precipitation** (mm)	**Return period** ($years$)
0.25	17.0	10
0.5	32.2	100
0.75	48.8	400
1	62.0	800
2	101.9	3000
3	121.1	3900
4	129.1	3600
5	133.4	3200
6	136.2	2900
12	147.4	1600
24	*166.0*	*1000*

Table 3.1 presents the maximal measured precipitation in millimeters and the calculated return period at different times registered during the rain duration. As can be seen, the return periods at the beginning of the rain (0.25 - 1 h) are significantly smaller and more varying than the rest of the rain (2 - 24 h). The greatest extent of return period is identified at a rain duration of 3 hours, reaching a value of 3 900 years. Furthermore, the return periods are determined according to the Station-year method (SMHI, 2021a), previously described in Section 2.3.1, and based on statistical data of the southeast (SE) and central (M) regions of Sweden. The data had removed outliers to make it more reliable. This means, however, that the measurements of the highest recorded precipitation are not included in the data set. Also, since the regional division of the data only was suitable for rain durations up to 12 hours, the italic values on the last table row are not as accurate (SMHI, 2021a).

The data that was collected from the five nearest VViS stations in relation to the case studies are presented in Figure 3.7. As can be seen it was raining heavily throughout that whole day of the 17th of August, and that it reached its heaviest load in the early evening of that same day.

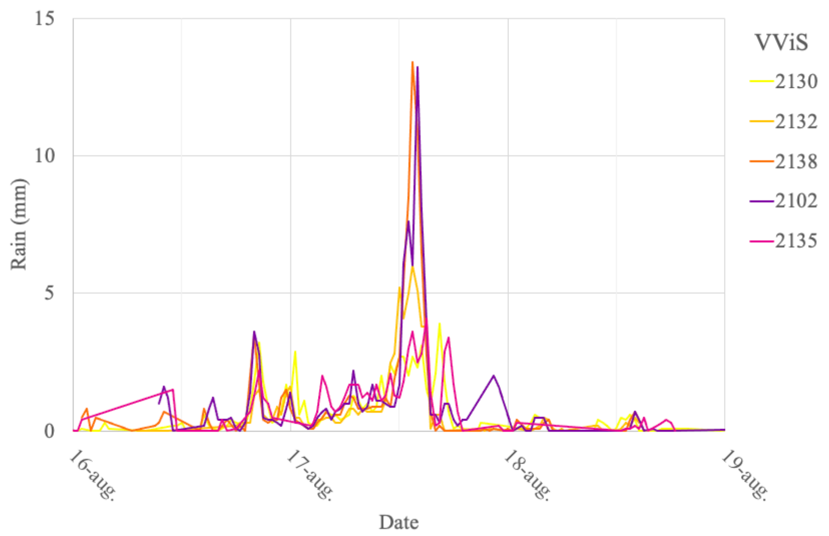

Figure 3.7: *The variation in precipitation measured during "Gävleregnet" at five VViS stations near the case studies, reaching a peak on the evening of the 17th of August 2021.*

But since hydrology is affected by more than one day of rain, it is important to review a broader view. In the following Figure 3.8, precipitation data of August 2021 according to SMHI (nda), is added for each day to present the total precipitation up to (and including) each individual day. The data is received from the nearest adjacent SMHI stations, and is indicated by the solid lines. The dashed lines describe the average precipitation of 1961-1991, plotted as a linear increase by assuming that this same amount of rain falls every day. The plot clearly illustrates that the SMHI weather stations have measured much greater amounts of precipitation compared to the statistically normal values for the month of August.

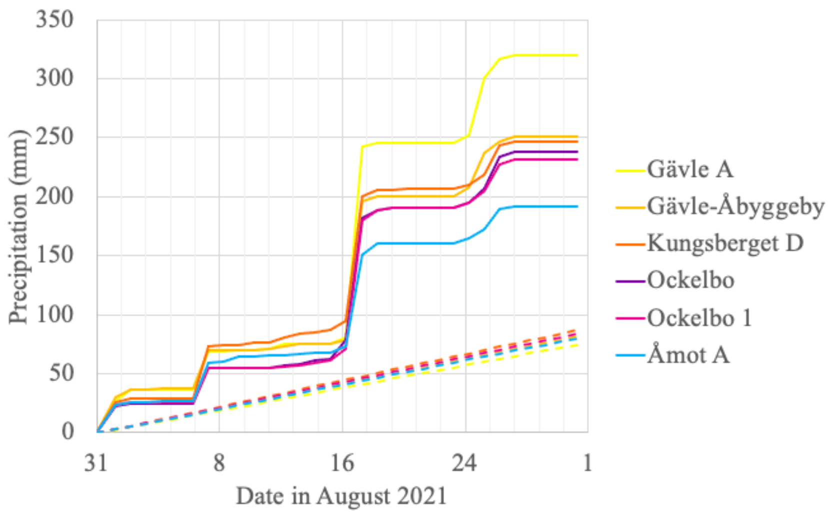

Figure 3.8: *Precipitation collected per day in August 2021 and in the closest located SMHI measuring stations, marked as solid lines and based on values according to SMHI (nda). The mean normal values between 1991-2020 according to SMHI (2021b) are marked as dashed lines.*

Additionally, Figure 3.9 below presents how the precipitation in July and August 2021 deviates from a statistically normal period of 1991-2020 according to SMHI (ndb). When analysing the deviation in August, it can be observed that the month contained around 250-300% of the statistically normal precipitation. The figure thus illustrates that all investigated SMHI stations have shown a very wet August. However, as also can be seen in the figure, the month of July was unusually dry in the Ockelbo area, where only 50-75% of the normal precipitation fell.

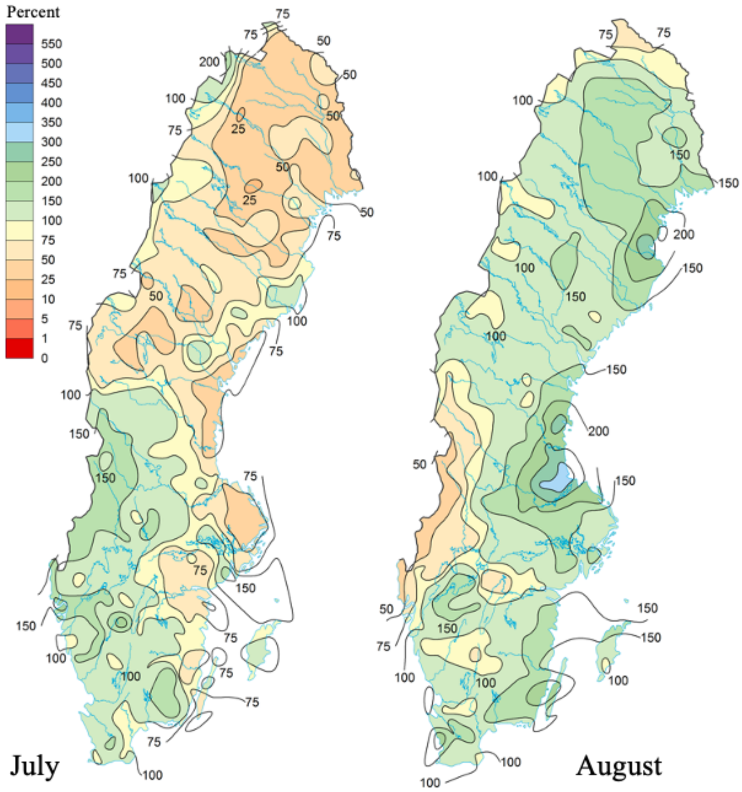

Figure 3.9: *Precipitation deviation in Sweden in July and August 2021, compared to a statistically normal period of 1991-2020 (SMHI, ndb).*

4 Methodology of the analysis and calculation processes

In this chapter, the execution of the performed analysis and calculation processes are explained. An overall description of the purpose and execution of the field visit is explained in Section 4.1. Section 4.2 describes the assessment of geographic and hydrographic input data for the given case studies and the process of evaluating them in GIS. The following section, 4.3, specifies the choices of the applied weather data for *Gävleregnet* and describes the two weather scenarios that have been analysed. The overall procedure for the manually performed calculations is described in Section 4.4 - 4.7, where the application of the Time-area method is described separately in the first section, followed by the remaining three sections presenting each of the three individual methods studied. The modelling in *Flödesappen* is described in Section 4.8. Finally, the utilization of the Colebrook's method and the executed sensitivity analysis are specified separately in the last two Sections, 4.9 and 4.10.

4.1 Field visit

To experience and gather more information about the case study areas, a field visit was executed on the 28th of April 2022. The late date in relation to the thesis work time, was due to the location of the case studies, where it is not uncommon to still have snow remaining in the beginning of May. During the visit, the in general characteristics of each case study was investigated to get a sense of how well the maps describe these areas. However, due to a limited time schedule, the visited areas and the observations made from them had to be considered as representative of all other comparable sites within the catchment areas.
A field checklist was summarized into following investigation points which were examined and exemplified during the site visit:

- Investigate the characteristics of the surroundings at the culvert pipes
- Investigate the characteristics of the creeks, ditches and roads
- Measure the water velocity of the creeks

For example, in Brattfors, the authors were interested to examine a branching in the main creek, that was found during review of the map in GIS. In Vallsbo, there were some uncertainties regarding the gravel roads of the area as there were some differences in how these roads were presented between different maps. Therefore, the authors decided to investigate them further.

4.1.1 The orange-test - Velocity measurements

The method that was utilized to estimate the water velocity on site was *Apelsintestet (eng. the orange-test)*. The test is a first estimation method that commonly is utilized by hydrogeologists (A. Gunnarsson, personal communication, April 28th 2022). The test could in practice be performed with any fruit or other inorganic thing/matter that fulfills the function of floating, but is heavy enough to float in the water instead of on the water.

In line with the description of the method by WWF (nd), the test was carried out by dropping an orange into the watercourse in question. When the orange hit the water surface the timing began, which then was carried out to a specific predetermined stop place. The distances were then measured, and a water velocity was calculated. Each water course was tested four times, two times for the two oranges. If the orange took a path that caused the orange to get stuck in branches or other vegetation, etc., then the experiment restarted. This can be regarded as removing of outliers. The velocity for each tested water course was then calculated as a mean value, that was deemed as a normal to a higher normal background flow, due to the season of spring flood was coming to an end.

The locations of the measurements were selected according to a few regulations. One thing that was important was that the conditions in the creek should be similar along the entire measuring distance. There was only one measurement opportunity in Vallsbo in the creek, and this measurement spot was downstream the culvert pipe, just after the outlet (V2). This happened because it was a small waterfall just upstream of the pipe which would have made the measurement conditions indeed very varied. In total the water velocity was measured at 6 different locations, as illustrated in Figure 4.1a, 4.1b, 4.2a and 4.2b, where two of those were at Vallsbo and the other four at Brattfors. The other measurement in Vallsbo was made through the pipe (V1). In Brattfors, the velocity was also measured through the pipe (B1), but also just upstream of the inlet (B2), at a branching upstream (B4) and between that branching and the culvert pipe (B3).

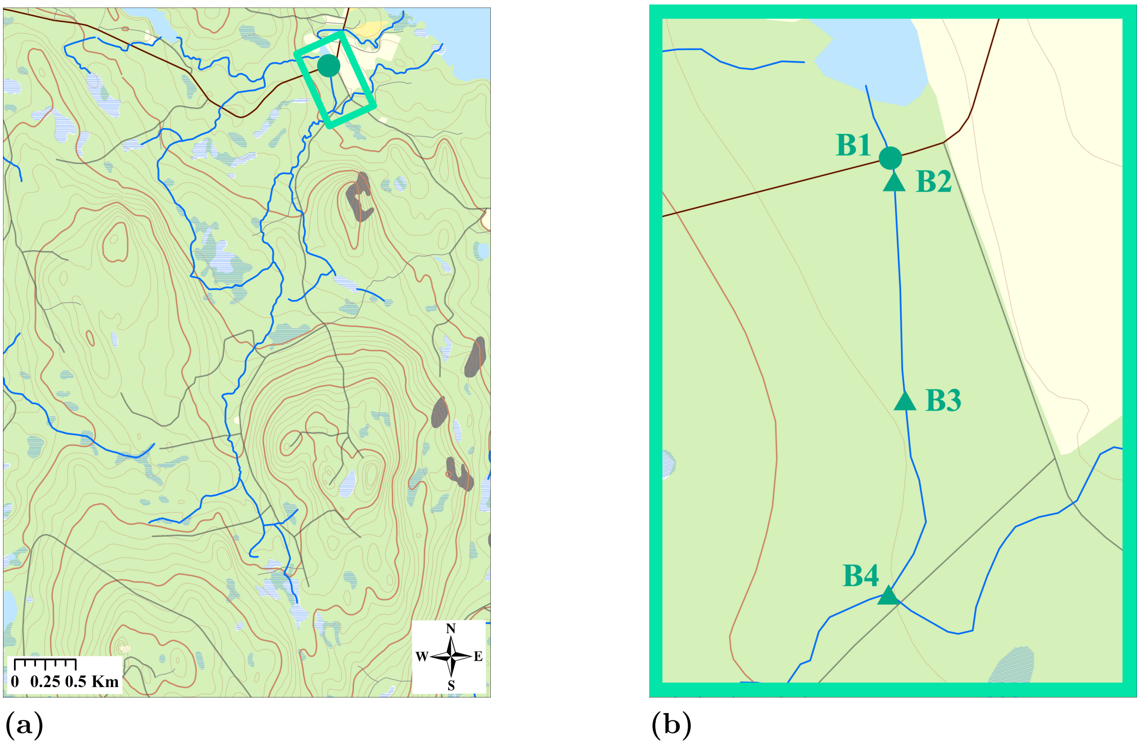

Figure 4.1: *The locations of the water velocity measurements in field for Brattfors.*

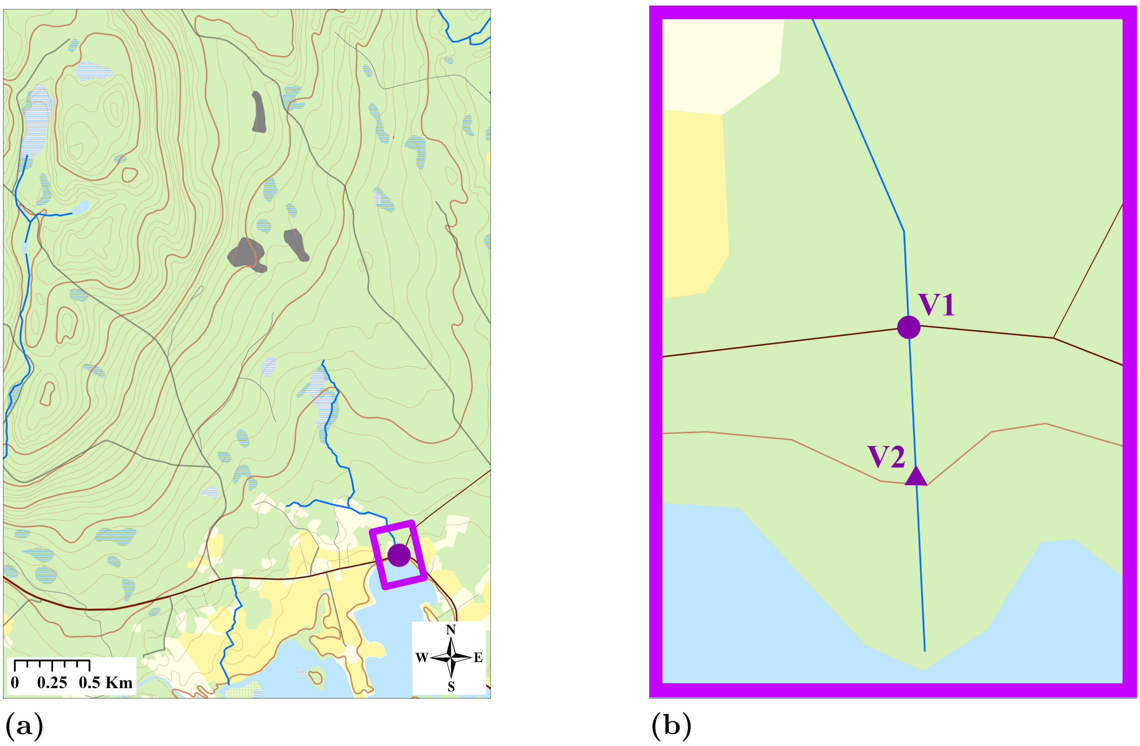

Figure 4.2: *The locations of the water velocity measurements in field for Vallsbo.*

4.2 Assessment of areal parameters

The program that was mainly used to analyse the terrains and assess the geographic and hydrographic characteristics of the catchment areas was the GIS program ArcGIS Pro 2.8. Compared to a manual approach with traditional maps, the calculations of catchment area and concentration time themselves could thus be performed more easily with regard to all data entered into the program. The raw data that was utilized was collected from the National Swedish Land Survey, and contained an elevation map, elevation contours, terrain map including information such as hydrographic lines, water surfaces, public and private roads.

The manual method of sketching an approximation of the total catchment area on a traditional/physical map, in this case printed from GIS, was made as a very first estimate to get an overview of the area before analysing it digitally. This was done by considering the elevation contours, of which the boundaries of the catchment area should be drawn perpendicular against. Thereafter, the total catchment area of each case study was further estimated and defined in GIS by identifying natural water dividers such as mountain peaks, or other inclined land surfaces and topographical ridges, as well as depression zones like rivers and creeks constituting natural barriers for water diversion and surface runoff in the landscape. These catchment areas were thereafter divided into smaller sub-areas with individually defined outlet points upstream the culvert pipes, to fulfill the desired requirement of receiving catchment areas covering no more than 80 ha in surface size (Chin, 2018), as described in Section 2.1.1. Similarly, but with regards to this size constrain, the sub-catchment areas were thus delimited as uniformly as possible considering different land types, inclinations and natural barriers in the landscape. Roads within the total catchment area were also, as far as possible, considered as water dividing barriers delimiting the different sub-areas.

Within each sub-catchment area, the longest runoff distance was defined according to a couple of assumed guidelines in order to receive the longest runoff time. Firstly, since runoff on vegetated land can be considered to be significantly slower compared with flows in road ditches or watercourses, the runoff was defined on vegetated land as far as possible within each area. This means, however, that the longest runoff time does not necessarily correspond to the longest possible runoff distance within an area; unless natural land covers most, or even all, of the longest runoff distance already. Secondly, it was assumed that wetlands constituted an end point for runoff pathways as water reaching these locations was assumed to be stored, having similar water storing properties as lakes and basins. Furthermore, runoff reaching roads was assumed to be gathered and diverted in ditches along the banks.

To facilitate the development of the catchment area and runoff pathways in GIS, latitudinal arrows created to represent in which direction the geographical formations in the landscape are inclined. A grid of 100x100 meters between each arrow was assumed to be most suitable for making the directions visible over the entire area in full scale. The goal of retrieving the catchment area in GIS was eventually accomplished by tracing a polygon at a separate layer according to elevation contours, assumed water dividing barriers and the retrieved latitudinal arrows. Moreover, SCALGO Live was also used to easily study profiles of different inclined sections, in order to estimate possible pathways more effectively for the runoff based on the same raw data from the National Swedish Land Survey. The longest runoff distance was thereafter estimated in GIS by creating a polyline along the longest stretch of latitudinal pointers that finally reaches the culvert pipe from a remote location, also with the help of supplementary analyses of corresponding profiles in SCALGO Live. Additionally, the gradient of the terrain along each longest runoff distance, used for the velocity calculations according to Svenskt Vatten, was estimated from profile charts of every individual stretch generated in GIS.

As a final step in the modelling carried out in GIS, the extent of different land covers in each sub-catchment area for both case studies were evaluated. More specifically, areas with wetlands, agricultural land and roads were estimated. The areas for both wetlands and agricultural land were automatically pre-calculated in GIS by the applied input data and were thus already available as attribute data. For these pre-defined polygons of wetlands and agricultural lands that were not entirely within the catchment areas but crossed or overlapped their boundaries, a visual assessment was made of the proportions belonging to each individual area. These proportions were then calculated separately based on the given attribute data. However, in contrast to the wetlands and agricultural land, the roads were predefined as polylines and thus only had pre-calculated lengths instead of areas. The roads also spread over several sub-catchment areas to a greater extent than the first two. Therefore, the extent of the road sections for each sub-area were estimated simply using the manual measurement tool in GIS. To then convert the lengths to an area, an asphalt road width of 4 meters and 2 meters was assumed for gravel roads located entirely within a catchment area, while half of these widths were assumed for the areas where the roads delimit two sub-areas.

4.3 Weather data

Weather data from both the Swedish Transport Administration's (STA) and the Swedish Meteorological and Hydrological Institute's (SMHI) measuring stations was available for the case studies in question. As mentioned in Section 2.3.2.1, weather data collected with the VViS is mainly developed and used for predicting the winter weather for the operation managers. Therefore, there are no special analyses already made on the raw data that can be collected from those stations. Considering the gained knowledge that the STA orders analysed weather data from SMHI when needed, the authors of this thesis have decided to use the already available SMHI information as they do not possess the ability to analyse weather data. This SMHI data is analysed and evaluated from the extreme weather *Gävleregnet* of 2021, and comes from a report obtained in consultation with the municipality of Gävle. The report is unfortunately unpublished as the document was requested and bought, but all raw data that the report utilized are available on SMHI's web page.

A disadvantage of using SMHI as data source compared with VVIS is that VViS stations are located closer to the current case studies, while the SMHI report was conducted for the city of Gävle. But since Gävle and Ockelbo are in close geographic relations and both are on the border between the short-term precipitation-regions described in Section 2.3.1, assumptions were made that the data from SMHI still would correspond to the case studies. Additionally, the VViS measurements of precipitation is not as accurate as the values retrieved by SMHI (see Section 2.3.2.1 and 2.3.2.2). It was therefore decided that the VViS data presented in Figure 3.7, will only be utilized as a verification of the SMHI data for the case study areas.

The SMHI data discussed above was first retrieved as presented in Table 3.1, then altered to fit the required form, which is presented in Table 4.1. The alterations transformed the precipitation measure and its unit of mm/time to a rain intensity and a unit of $l/(s \cdot ha)$. This was accomplished by multiplying the precipitation by 10 000 cubic meters per hectare and then dividing by the time interval in seconds. For derived unit conversion, see Appendix B. The rain intensity is presented in Table 4.1 and plotted in Figure 4.3 together with the IDF national mean curves, previously mentioned in Section 2.1.1 and Figure 2.1.

Table 4.1: *The calculated rain intensity ($l/(s \cdot ha)$) for the "Gävleregnet 2021". The values are calculated from the given values in Table 3.1 which was collected from SMHI (2021a).*

Rain duration (h)	**Rain Intensity** ($l/(s \cdot ha)$)
0.25	188.9
0.5	178.9
0.75	180.7
1	172.2
2	141.5
3	112.1
4	89.7
5	74.1
6	63.1
12	34.1
24	*19.2*

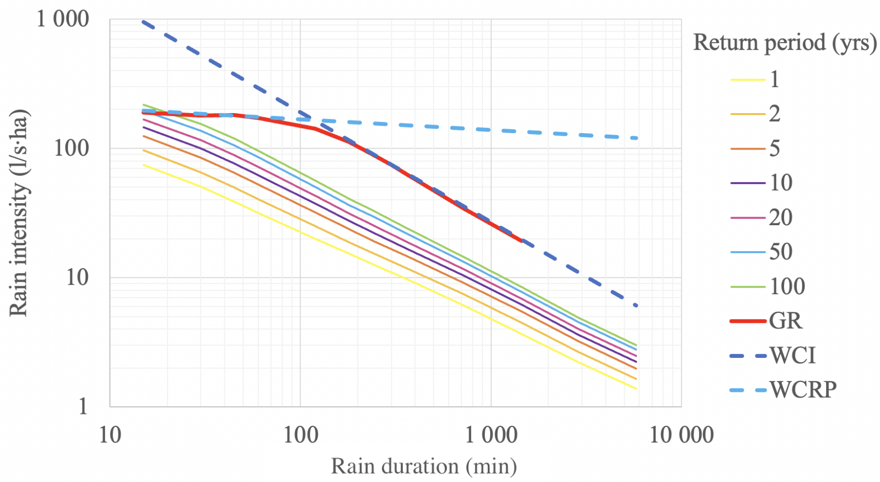

Figure 4.3: *The rain intensity of the Gävleregnet (GR) and Gävleregnet extrapolated for short and long rain durations, plotted together with the mean (reduced) rain intensity for Sweden and different return time intervals according to (Dahlström, 2006). The type of diagram is usually referred to as a IDF plot. Values for GR are produced from the data in Table 3.1. Authors' own work.*

When considering the red curve of the real rain event in Figure 4.3, two extrapolated trends become apparent, which are marked as the dark and light blue dashed lines. The light blue trend line illustrates that an extrapolation of short and intense rainfall over time corresponds to a significantly greater variation in return period seen over the entire rain event. In contrast, the dark blue extrapolation of the prolonged rain durations with higher return periods corresponds to a significantly greater variation in rain intensity, also seen over the entire event. The first mentioned trend line can therefore be considered as "the Worst Case of Return Period" (WCRP), and the latter trend line as "the Worst Case of rain Intensity" (WCI). It can further be seen that WCRP depicts a heavy rain that lasts a long time, while WCI depicts a heavy rain with has a much higher intensity in the beginning that then decreases. The analysed scenarios could therefore be seen as the flow effects of a heavy long-term rain versus the effects of downpour that is more intense but during a shorter time.

A knowledge that motivates the value of investigating two such rain scenarios is that impervious areas contribute to a greater runoff than permeable surfaces at shorter rain durations. But for rains with greater durations, permeable surfaces can generally get a greater surface runoff as permeable soils get moisture saturated. The two rain scenarios that were selected for this thesis are therefore the WCI and WCRP, as described above.

Additionally, based on the weather conditions of the studied rain event described in Section 3.3, the soil was assumed to have already been saturated with moisture at the time when the heavy rainfall began. In the calculations, this assumption thus means that the proportion of the rain that becomes runoff (depending on the runoff coefficient) has been considered to flow directly as runoff when the rain falls on the ground.

4.4 Time-area method

As described in the Chapter *2 Theory*, the Time-area method (T-A) should be used when the total catchment area exceeds a certain areal requirement. Thus, the runoff within each sub-catchment area will still be calculated separately for each variant of the Rational Method (RM), and then the use of the isochrones as described in Section 2.1.4 is applied to receive the total runoff to the culvert pipe when all sub-areas contribute together.

More in detail, after the sub-catchment areas were divided according to the description in Section 4.2, the reduced areas were calculated by multiplying the runoff coefficient with the area for each respective sub-catchment and each respective method (RM, SV-RM and STA-RM). And the longest runoff times were also calculated in line with what each specific method dictated. Thereafter, isochrones were generated by plotting each reduced area to the runoff time, which is used to illustrate the time it takes for each sub-area to contribute to runoff with its maximum capacity. All isochrones were then added together forming the Time-area Histogram (TAH) to get the total runoff from the reduced area to time. The total reduced area at the time of each breaking point in the TAH-curve was thereafter multiplied with the corresponding rain intensity for that point. Since the report investigates two different weather rain scenarios, two different flow curves were thus finally generated for each method and case study.

As a remark specific to the application of the T-A for these two case studies is that no consideration needs to be given to parallel shifting of the TAH as described in Section 2.1.4. The reason why parallel shifting is that the calculation points of the case studies (the culvert pipes) are directly connected to the catchment areas. There is thus no transport distance, for example in the form of a pipe, through which the rainwater must travel before the area can begin to contribute to runoff. Therefore, it is assumed that the sub-areas in which the calculation points are located begins to contribute directly to the run-off when the rain starts to fall, which may reflect that in reality precipitation falls straight down in front of the culvert pipes' inlet.

4.5 Rational Method

To calculate the flow using the Rational Method (RM), a few assumptions and other calculations are needed to be determined first. The overall method is described previously in Section 4.4.

For the RM it was decided only to consider the following land covers: forested land, exposed bedrock, agricultural land, wetland and lake area. Since the road surfaces was evaluated to less than 1% of the total area their impact were deemed disregarded. The total catchment area and sub-catchment areas was assumed as described in Section 4.2 and 4.4.

As mentioned in Section 4.4, the runoff coefficient for the total areas was calculated according to Equation 2.2 with land cover values according to Table 2.1. The selected values for each land cover were 0.3 for exposed bedrock, 0.1 for forested land, agricultural land and wetland.

The longest runoff distance was decided in accordance with Section 4.2. These values were then utilized together with the Table 2.3 to calculate the longest runoff time according to Equation 2.4. To calculate the flow using Equation 2.1, the summation of isochrone plots was multiplied with the rain intensities, as described in 4.4.

4.6 Svenskt Vatten

As described in Section 2.1.2, an estimation method of natural land flows is presented by SV (2016), which is based on a diagram for natural land runoff as a function of area size and rain return period. Due to several factors, that approach was not applied in the flow calculations within this thesis. The main factors were that even the highest available return period in the diagram was considered as too low to be compared with the studied rain event, and that the data originates from observations made in the southwestern Sweden. Consideration of the impact of natural land runoff has therefore only been taken into account by using low runoff coefficients to represent the natural land, which is also recommended by SV (2016).

4.6.1 Water velocity utilizing Manning's equation

The investigated land covers are assumed as described in Section 4.5, with the same assumptions for the road areas and runoff coefficients. What was differentiated from the RM methodology was the calculation of the longest runoff time. The data and general equation presented in Section 2.1.2, Equation 2.4, was the same, but instead of assuming water velocities from Table 2.3, they were calculated according to Equation 2.6 - Manning's equation.

Firstly, the runoff was divided into four different types: exposed bedrock, land (soil), ditch and creek. For the exposed bedrock and land, the hydraulic radius (R) was only corresponding to the water depth since the width is assumed to be infinitely large for water flowing on the ground surface. Thereafter, the Manning's coefficient (M) was selected for each type of runoff based on Table 2.6, but with some adjustments. The coefficients were chosen equal to Table 2.6 for land (assessed as bush field), ditches (specified with some vegetation) and exposed bedrock (assumed as similar to coarse concrete in constructed coated canals). This led to values of M = 25 for ditches, 5 for land and 50 for exposed bedrock. However, a more conservative value was chosen for the creeks, which during the extreme rain event can be expected to have had high water flows. A value of 35 for Brattfors and 30 for Vallsbo, just above the highest for creeks, was therefore chosen. Furthermore, the water depth for the runoff water on exposed bedrock and land was assumed to 5 cm. For the creeks and ditches, the wet perimeter was calculated by assumptions of their geometry made in field, these are presented later on in Chapter 5, Figure 5.1 and Table 5.1. They were also assumed to be completely filled with water, which meant that the water depth became equal to the estimated creek depth. Lastly, before finalising the calculation with Manning's equation, the gradients of the area along the longest runoff distances was estimated based on the profiles of these obtained from the GIS analysis.

The maximal flow was calculated by multiplying the reduced area with the rain intensity and climate factor for each respective time laps. The climate factor was retrieved from Table 2.4. The pipe dimension was then scaled up, according to Equation 2.10, so that the calculated flow only filled 85% of the suitable culvert pipe.

4.7 The Swedish Transport Administration

Initially, the authors had the intention of dividing the sub-catchments further, to include the specific runoff flow for road and near road surfaces (Equation 2.8) that the STA mentions in their guidelines TRV INFRA and MB310. But since the road areas were presumed to constitute less than 1% of the catchment areas, the same presumptions were used as in RM and SV-RM when determining the runoff factor and reduced area respectively, thus without explicit consideration of infiltration capacity.

The longest runoff time is calculated in a similar manner as in Section 4.5. But instead of utilizing Table 2.3, Table 2.7 was employed. The method recognized different water velocities for creeks, dikes, soil and exposed bedrock. Where the creeks assumed a velocity of 0.5 m/s, 0.2 m/s for ditches, 0.1 for land and 1.5 for exposed bedrock.

When a reduced area and longest runoff time for each sub-catchment area were achieved, the isochron and the summation of isochron were plotted. To retrieve the dimensioning flow, the rain intensity and the reduced area were multiplied with the climate factor retrieved from Table 2.4. Just as for SV-RM, STA-RM assumed a filling degree of 85%.

4.8 Flödesappen

To estimate the catchment area of each case study in *Flödesappen*, the pin was placed in each creek just upstream of the culvert pipe. In Brattfors, the hydrograph-line was incomplete in relation to the real pathway and branching of the creek. To overcome this issue, the pin was placed on three other hydrograph-lines in the known water direction. This created three individual parts that was summarized into one area, depicting an estimation of the total catchment area in Brattfors. However, since there was no issue with the hydrograph-lines in Vallsbo, the total catchment area was estimated as intended with only one pinpointing. Furthermore, the shares of the different land covers for each estimated catchment area were obtained. The different percentiles of the individual parts in Brattfors were consequently combined into a total share to describe the land covering within the estimated total catchment area.

As mentioned in Section 2.1.5, the runoff flow can in *Flödesappen* be calculated automatically according to MB310, TRVINFRA and RM respectively. But none of these methods could be applied for all pinned catchments, as some needed values were not obtained or could not be obtained, for example due to that the lowest permitted areal size was not reached. It was therefore decided to not perform any flow calculations in *Flödesappen*, since they could not be made comparable to each other or to any of the manually calculated flow results of the RM versions. Thus, only the catchment areas and their areal parameters estimated in *Flödesappen* were compared with the corresponding results of the assessment in GIS and the manually performed calculations.

4.9 Colebrook's method

The calculated dimensioning flow and the arbitrary gradient of 5 ‰ was utilized to determine a suitable pipe dimension with Colebrook's diagrams, which was done for all manually performed methods (i.e. for RM, SV-RM and STA-RM). The roughness was decided according to corresponding culvert pipe materials in Table 2.13. For RM and SV-RM, this resulted in 1.0 mm for the concrete pipe in Vallsbo and the 0.2 mm for the trenchcoat pipe in Brattfors since there is no Colebrook diagram available for roughness's as fine as 0.05 mm. But since STA (2021a) have specified that no roughness below 1.0 mm should be utilized in any case, the calculation method STA-RM utilized 1.0 mm for both case studies. Additionally, Colebrook's diagram for roughness 0.2 is available in Appendix A.

4.10 Sensitivity Analysis

It was decided to investigate the impact that some assumed factors had on the results. Following factors were considered; the runoff coefficient, the water velocity, the sub-catchment areas and the Manning's coefficient. These factors were selected due to their suggestiveness, that it generalizes and potential inaccuracy. The sensitivity analysis was conducted by increasing the factors by a percentage, *ceteris paribus*, to investigate the impact of each increased parameter to the change in dimensioning flow.

The increase of the runoff coefficient was selected to mimic the result of the land being water saturated. This was done by increasing the runoff coefficient of forested land surfaces by 200%, from 0.1 to 0.2. Another way to resemble the land being saturated was to increase the water velocity on land surfaces, this was done by increasing the velocity by 300%, from 0.1 m/s to 0.3 m/s.

Since the water velocity is calculated for SV-RM, the creek's velocity was increased by 150%. The sub-catchment areas were investigated by decreasing the size of the sub-catchment areas to the limit of 30 ha. Since some of the calculated sub-areas measured 80 ha, the decreasing of the areas was 62.5%, which means that they were multiplied by 0.375. This was due to the decision to of assuming the areal limit of 80 ha according Chin (2018) to instead of 30 ha according to SV (2016). The longest runoff distances were also multiplied with the same factor, to match the new catchment sizes. To investigate Manning's coefficient, the factors for the creeks, ditches, soil and exposed bedrock were increased to 150% of its original.

5

Results

This chapter presents the obtained results of the case study analyses and each sensitivity analysis, divided into the following six sections. The gained knowledge from the field visit is described in Section 5.1, whereas the areal parameters assessed from the GIS analysis are presented in Section 5.2. Section 5.4 presents the estimated water velocities, followed by the results of the dimensioning flows and corresponding culvert pipe dimensions in Section 5.5. Finally, the outcomes of the sensitivity analysis are given in Section 5.6.

5.1 Field visit

This section presents the discoveries and observations of the case study areas and their area-specific characteristics made in field. These, which are described in the following three Sections 5.1.1 - 5.1.3, provided valuable input to the analysis performed in GIS.

5.1.1 Discoveries affecting catchment area boundaries

The first discovery made in field for Brattfors was registered in the creek about 350 m upstream of the culvert pipe. There in the branching of the creek, it turned out that the flow path leading water to lake Hammarsjön was dammed. Water could therefore no longer pass the adjacent gravel road through an existing smaller culvert pipe. Moreover, a lowering zone was observed along the opposite side of the gravel road in relation to the dam point. The runoff that according to the directions of the latitudinal arrows in GIS was thought to flow from a peak and all the way to the road will in reality stop at the depression in between. This difference in elevation thus means that water flows off the road in the direction away from the creek rather than towards it. As a result, the boundary of the catchment area was reshaped to instead follow the road for about 950 m, from the dam point to the next culvert pipe passage where the creek crosses the road. The number of sub-areas was hence reduced from 13 to 12 compared to the initial estimation. Apart from some small adjustments, no further major change was made to the total catchment area thereafter.

In Vallsbo, three smaller culvert pipes were discovered along the asphalted road X456. The boundary that extends along this stretch of road of about 1 km from the studied culvert pipe was therefore shortened down to about 200 m, to the nearest smaller culvert pipe, which resulted in a significantly reduced catchment area. Furthermore, it turned out that the smaller road connecting to the visited gravel road was a shift road, probably was used as a passage for forest machines and other similar heavier vehicles. This was assumed since it was observed as slightly depressed in relation to the surrounding terrain. The shift road itself could therefore be seen as a low point diverting runoff back to the larger gravel road. As the same conditions were assumed to apply to the other adjacent shift road, this observation resulted in a further division of catchment area. In total, together with the discovery of the smaller culvert pipes, the total catchment became reduced but the change of the boundaries resulted in an increase of the number of sub-areas.

5.1.2 Area-specific observations - Ditches

After the discovery of the dam, the inspection in Brattfors continued along the adjacent gravel road until the wind farm was reached at the intersection a few kilometers further into the catchment area, by point B4 in Figure 4.1b. The ditches along this stretch were generally vegetated, and were estimated to be 0.2-0.5 m deep and a maximum of 0.5 m wide. However, at the reached intersection, the elevation between the road and the ditches was leveled out. Water can thus be assumed to flow across the road at such an intersection.

The ditches along the visited gravel road in Vallsbo were assumed to have the same dimensions as in Brattfors. As they also were leveled out at the intersection close to the shift roads, the same assumption applies that water crosses the intersection on its surface. No ditches were observed at the shift road, but as mentioned earlier, the shift roads themselves could be assumed to transport water due to their slightly depressed shapes. However, since the properties of a road differ from a ditch in terms of size (width and depth), such a transport can be comparable to runoff on soil.

5.1.3 Area-specific observations - Creeks

The geometry of the creek in Brattfors was assessed when inspecting the branching stretching from the dam point to the culvert pipe. The closer to the culvert pipe, the narrower and shallower the creek became. Overall, it was estimated to be 1.5-3 m wide, with a creek depth varying from 0.5-1 m and a water depth about 0.2 m at the shallow sections and 0.5 at the deep ones. The flow conditions were generally calm, and the bed of the creek consisted mostly of rocks as hardly any vegetation was observed.

In Vallsbo, the creek was only observed at the studied culvert pipe. As mentioned in Section 4.1.1, velocity measurements were only performed downstream of the culvert pipe, where the dimensions of the creek were estimated to approximately 1.5 m wide and 0.5 m in creek depth. Seen from the inlet of the culvert pipe, the dimensions seemed to be similar upstream. But, as the water rushed down a more inclined terrain, the flow conditions were much more turbulent compared to the flat and calmer conditions downstream where the creek also opens into lake Vallsjön.

The characteristics of the creeks and ditches of the area was afterwards summarized to mean widths, water depths and shapes. These are presented in Figure 5.1 and Table 5.1 below.

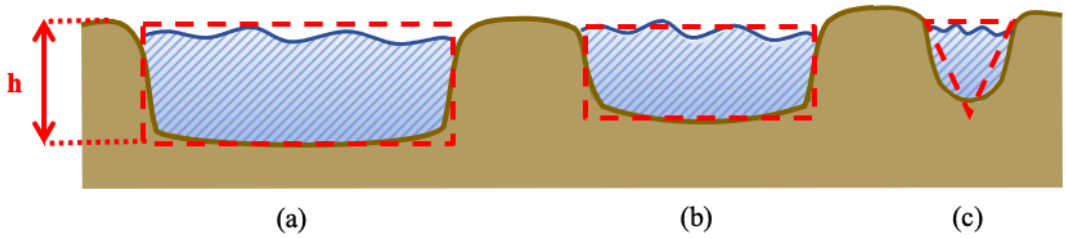

Figure 5.1: *An illustration of the presumed cross sections of the case study areas. The h represents the creek depth. The watercourse to the far left, (a), is the assumed creek cross section for Brattfors. The illustration in the middle, (b), is the creek in Vallsbo, and the illustration to the right, (c), is the assumed ditches throughout the two case studies. The assumed dimensions of the water courses are presented below in Table 5.1.*

Table 5.1: *The assumed dimensions of the water courses for this thesis.*

Parameter	Watercourse		
	Brattfors Creek	**Vallsbo Creek**	**Ditch**
Width (m)	2.3	1.5	0.4
Creek Depth (m)	0.75	0.5	0.25

5.2 Areal parameters in GIS

The catchment areas assessed in GIS for each case study are shown in Figure 5.2a and 5.2b below. The bright coloured dashed lines describe the initial division of the catchment areas whereas the darker solid lines portray the final shapes and boundaries adjusted after the gained knowledge from the field visit. The locations of the studied culvert pipes are marked by the darker coloured dots while the brighter dots correspond to the position of the inventoried smaller culvert pipes. In contrast to the ones in Vallsbo, the smaller pipes in Brattfors were already inventoried before the field visit. Additionally, the estimated longest runoff distances are shown separately for each case in Figure 5.3a and 5.3b and in Figure 5.4a and 5.4b respectively. They are color-coded for each sub-area, where the outlet point of each area is marked with a square filled in with matching colour.

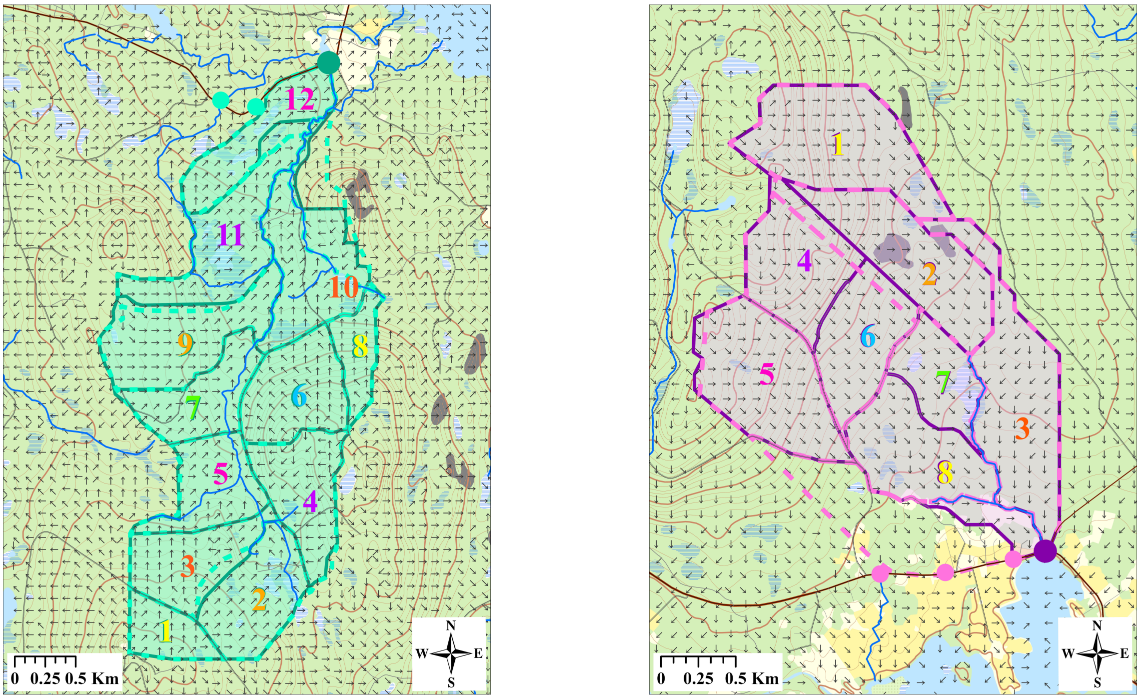

(a) **(b)**

Figure 5.2: *The estimated and divided catchment area for the culvert pipe of each case study; Brattfors to the left (a), and Vallsbo to the right (b).*

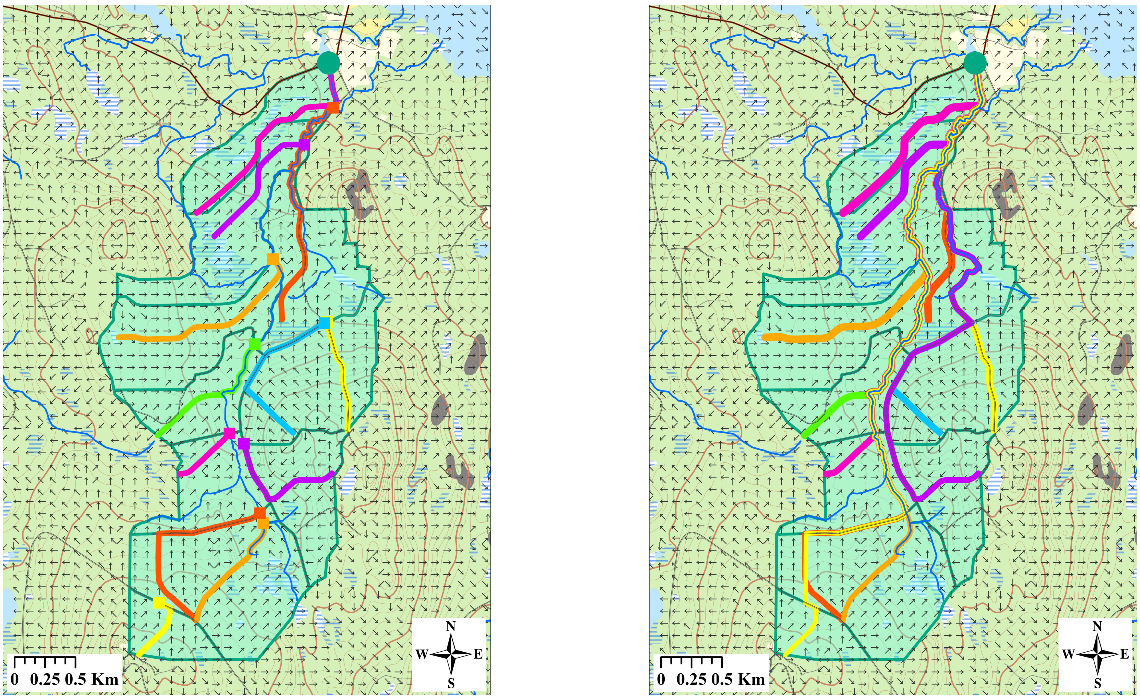

(a) **(b)**

Figure 5.3: *The longest runoff distances in Brattfors; Within each sub-catchment area to the left (a), and the total to the right (b).*

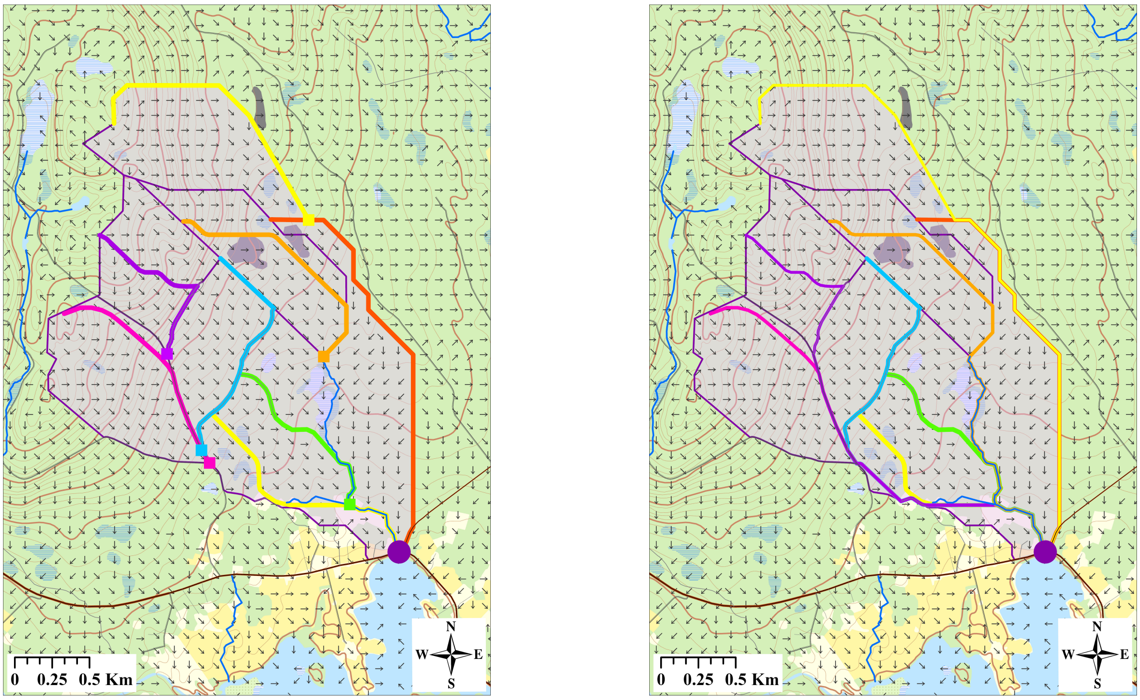

(a) (b)

Figure 5.4: *The longest runoff distances in Vallsbo; Within each sub-catchment area to the left (a), and the total to the right (b).*

The results of the areal parameters, sub-catchment areas and longest runoff distance, in Brattfors are presented in Table 5.2 below.

Table 5.2: *The calculated sub-catchment areas and longest runoff distances in Brattfors.*

Sub-catchment	**Area** (*ha*)	**Longest runoff distance** **Within area** (*m*)	**Total** (*m*)
1	28	582	6 576
2	62	1 019	5 678
3	56	1 695	6 267
4	58	1 099	5 268
5	51	541	4 368
6	62	1 412	4 265
7	51	1 211	4 148
8	27	921	3 745
9	80	1 672	3 785
10	80	2 170	2 550
11	80	1 460	2 083
12	49	1 898	1 898
Total	685		

As can be seen in Table 5.2, three of the 12 sub-catchment areas are in the upmost areal limit of 80 ha each, whereas the smallest area corresponds to 28 ha. The longest runoff distances within the sub-areas varies between 541 m to 2 170 m, and the total distance to the studied culvert pipe varies between 1 898 m and 6 576 m. Furthermore, the shortest of the longest total runoff distances is given for sub-catchment 12, in which the total is equal to the distance within area.

In Table 5.3 the land covers according to the Swedish Land survey are presented for Brattfors. The table presents that a very great majority of the land is forested land. Unfortunately, the Swedish Land survey does not present any variation on the forested land-category in the map that this thesis utilized. For example, it does not say if the forested land was clear-felled or forested wetland.

Table 5.3: *The land covers of the assumed catchment area in Brattfors according to the Swedish Land Survey, prepared in GIS.*

Land cover	**Share** (%)
Developed land	0.5
Forested land	93.5
Wetland	6.0
Agricultural land	0
Exposed bedrock	0

The sizes of the sub-catchment areas in Vallsbo, as well as their longest runoff distance within each area and in total, are presented in Table 5.4 below. None of the 8 sub-catchment areas in Vallsbo touch the areal limit of 80 ha, but there are three sub-areas reaching over 70 ha where the largest of these corresponds to 77 ha. The smallest area measures 31 ha. Furthermore, the longest runoff distances vary between 1 286 m and 2 858 m, and the total runoff distances differ between 1 796 m and 4 606 m.

Table 5.4: *The calculated sub-catchment areas and longest runoff distances in Vallsbo.*

Sub-catchment	**Area** (*ha*)	**Longest runoff distance**	
		Within area (*m*)	**Total** (*m*)
1	74	2 001	4 606
2	61	1 712	3 411
3	77	2 858	2 858
4	51	1 286	3 659
5	71	1 560	3 140
6	45	1 622	3 310
7	31	1 322	1 857
8	65	1 796	1 796
Total	476		

As can be seen when comparing Table 5.2 and 5.4, the total catchment area in Brattfors is almost 150 % larger then in Vallsbo, which is also illustrated by the need of more sub-catchment areas in Brattfors to stay within the areal limit.

In the following Table 5.5 the different land covers for Vallsbo presented. The catchment area consists of 5 different land types, the smallest of them being agricultural land and the greatest forested land. In relation to the results shown for Brattfors is it illustrated here that a greater variation was detectable for Vallsbo on the Swedish Land Survey map utilized.

Table 5.5: *The land covers of the assumed catchment area in Vallsbo according to the Swedish Land Survey, prepared in GIS.*

Land cover	**Share** (%)
Developed land	0.8
Forested land	82.8
Wetland	2.2
Agricultural land	0.4
Exposed bedrock	1.3

5.2.1 Exceptions within the defined catchment areas

As mentioned in Section 4.2, roads within the catchment areas were as far as possible assumed to be water dividing barriers affecting the division of sub-areas. This means that runoff reaching the roads becomes transported in the ditches along their distribution. However, for some sub-areas, exceptions of this had to be made in order to estimate possible runoff pathways to the culvert pipe. In Brattfors, one exception had to be made for the stretch of the road that delineates sub-catchment area 1. As no water otherwise would be able to cross this road section, the runoff was assumed to flow over at its lowest point identified using the profile tool in SCALGO Live. A probable scenario in reality could then be that rainwater accumulates at the low point and eventually crosses the road. Therefore, as shown in Figure 5.3b, the longest total runoff distance for sub-area 1 crosses the road at where this low point is identified, which also thus corresponds to the defined outlet point.

Furthermore, a similar exception as above was made in Vallsbo, at the intersection of the gravel road where sub-area 4,5 and 6 meet. Due to the leveling of the ditches as described in Section 5.1.2, some of the runoff transported to this point can be assumed to flow off the road and continue on the land surface. This explains why the longest total runoff distances for these three latter sub-areas deviate from the road at the intersection instead of following along the gravel road's distribution (see Figure 5.4a).

When estimating the gradient of the terrain along the longest runoff distances, there were a few inaccuracies appearing in some of the generated profile charts in GIS which had to be disregarded. Generally, the defined pathways for runoff usually corresponded with a declining gradient throughout the whole stretch in the profile charts, which the gradient of the longest runoff pathway for sub-area 5 in Vallsbo exemplifies in Figure 5.5a. However, some profiles indicated on smaller sections of ascending inclinations along the runoff distance as Figure 5.5b shows for sub-area 10 in Brattfors. In the figure, this is specifically visible from about 1 200 m in the horizontal direction, which corresponds to where the runoff ends up in the creek for this defined stretch.

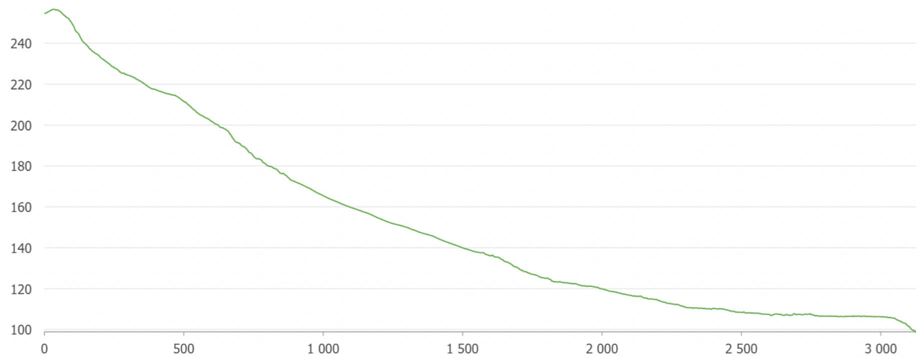

(a)

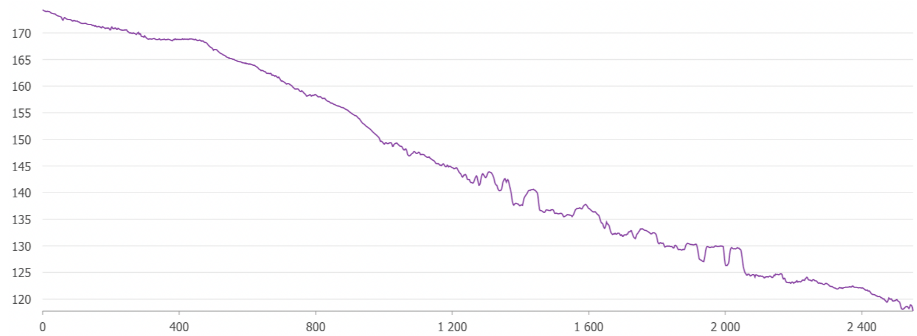

(b)

Figure 5.5: *The plots present two profiles of the longest runoff distances produced in GIS, (a) presents a desirable and gradually declining silhouette which was produces for sub-catchment 5 of Vallsbo and (b) presents a less ideal profile that was produced for sub-catchment 10 of Brattfors.*

5.3 Areal parameters in Flödesappen

In the following section, the results from *Flödesappen* are presented, starting with Brattfors and finishing with Vallsbo. The catchment areas' shape and areal sizes as well as the longest runoff distances and land covers are presented.

Since the hydrograph-lines of the creek in Brattfors were not completely correspondent to the reality, as mentioned in Section 4.8, the catchment area in Brattfors was depicted by summarizing three individual parts into one total area. These three areas (part 1, 2 and 3) are shown in Figure 5.6a, 5.6b and 5.6c respectively. Their different sizes and longest runoff distances are presented in Tabular 5.6 below, together with the estimated total catchment area in italic writing on the last row. It reaches a total size of 650 ha.

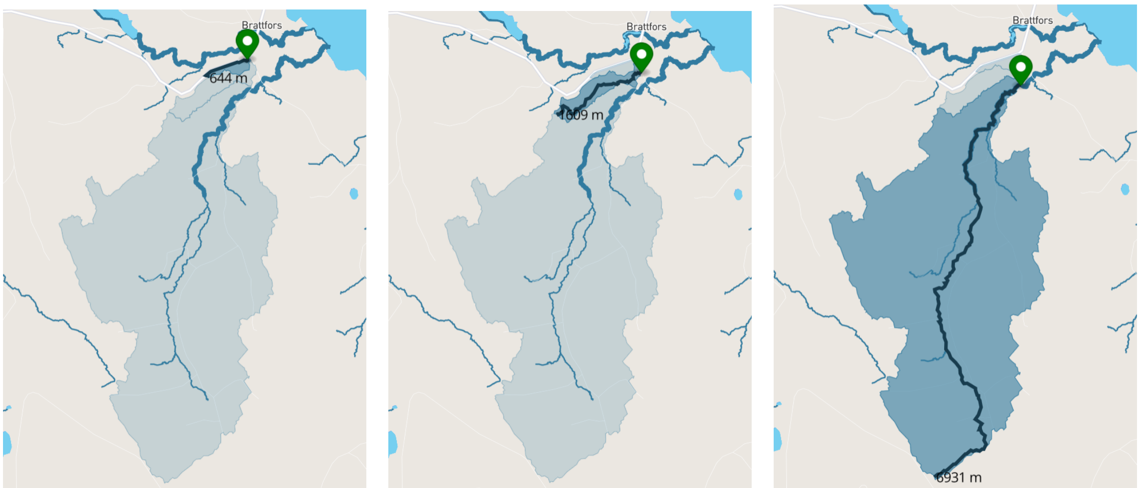

(a) **(b)** **(c)**

Figure 5.6: *The three parts that together make up the total catchment area of the culvert pipe in Brattfors, estimated in Flödesappen. To the left, part 1 is presented, followed by part 2 in the middle and part 3 to the right.*

Table 5.6: *The calculated area and longest runoff distance of each part of the total catchment area in Brattfors, estimated in Flödesappen.*

Part	**Area** (ha)	**Longest runoff distance** (m)
1	5	644
2	19	1 609
3	626	6 931
Total	*650*	

The percentiles of different types of land covering for the three smaller catchments in Brattfors are summarized and presented in Table 5.7 to describe the total catchment area. As can be seen, there are five different land covers presented, where the two largest shares are two types of woodlands; clear-felled area and forested land.

Table 5.7: *The land covers of the catchment area in Brattfors, estimated in Flödesappen.*

Land cover	**Share** (%)
Developed land	2.0
Clear-felled land	28.7
Forested land	61.6
Forested wetland	0
Wetland	1.8
Agricultural land	0
Open land	0.8
Exposed bedrock	0

In Vallsbo, there was no issue with pinpointing the hydrograph-line corresponding to the creek, as also mentioned in Section 2.1.5. Figure 5.7 shows the catchment area of the culvert pipe. Its total surface area and longest runoff distance are further presented in Table 5.8. The catchment area reaches a total size of 375 ha.

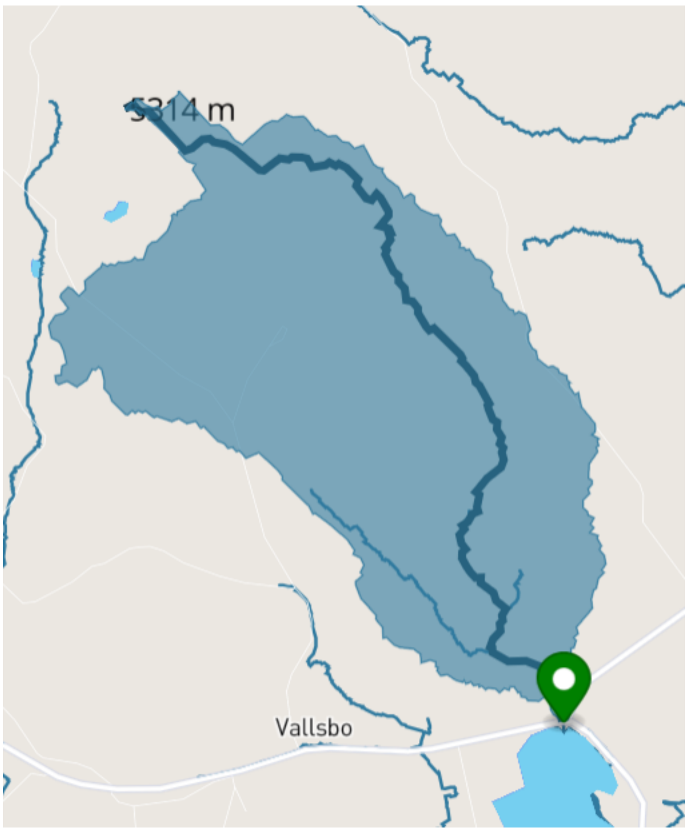

Figure 5.7: *The catchment area of the culvert pipe in Vallsbo estimated in Flödesappen.*

Table 5.8: *The size of the catchment area in Vallsbo and the longest runoff distance.*

Part	**Area** (*ha*)	**Longest runoff distance** (*m*)
Total	375	5 316

The land covers of the estimated catchment area in Vallsbo are presented in Table 5.9. And as can be seen, all of the eight different land covers are present, where forested land and clear-felled areas correspond to the largest shares. The smallest recorded share is Exposed bedrock which only represents 0.01 % of the total.

Table 5.9: *The land covers of the catchment area in Vallsbo, estimated in Flödesappen.*

Land cover	**Share** (%)
Developed land	1.3
Clear-felled land	18.6
Forested land	74.4
Forested wetland	2.6
Wetland	1.2
Agricultural land	1.0
Open land	0.9
Exposed bedrock	0.01

5.4 Calculated water velocities in the creeks

The measured and calculated water velocities are presented in Figure 5.8, where the green icons are the result for Brattfors and the purple for Vallsbo. The icons presented by circles and triangles correspond to the velocities measured in field, where the circles symbolize the measurements through the culvert pipes while the triangles represent the velocities from measurements in the creeks. Each location of the measurements is clarified in Figure 4.1a and 4.1b for Brattfors and in Figure 4.2a and 4.2b for Vallsbo. Additionally, the crosses represent all the calculated velocities for *Gävleregnet* in the creeks according to the method by Svenskt Vatten method (Manning's equation), and the green dashed line is the tabulated value for water velocity mentioned by Lyngfelt (1981); SV (2016); Bondelind and Häggström (2018), among others.

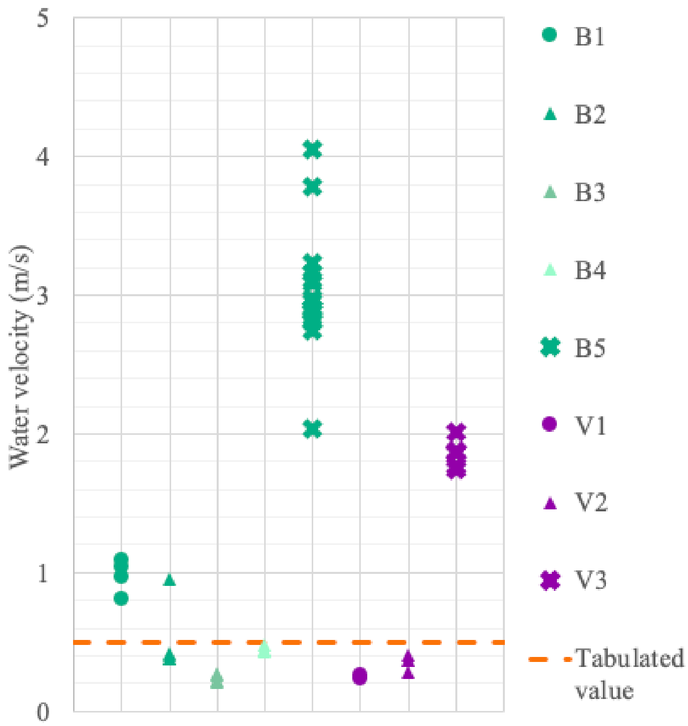

Figure 5.8: *The measured water velocity in the creeks (triangles), measured Water velocities in the pipes (circles) and calculated (crosses) water velocities in creeks for the two case studies, compared to the tabulated value for water velocity in streams.*

In Figure 5.8, it is apparent that the calculated velocities in the creeks, marked with coloured crosses, are much higher than both the measured velocities in field, marked in circles and triangles, as well as the tabulated velocity value. The calculated velocities in Brattfors are also higher and have a larger spread compared to the calculated velocities in Vallsbo.

5.5 Dimensioning flows and culvert pipe dimensions

The calculated flows over time for Brattfors are shown in Figure 5.9. These are presented for the three investigated applications of the Rational Method; the Rational Method (RM), Svenskt Vatten (SV-RM) and according to the Swedish Transport Administration (STA-RM), as well as for the two rain scenarios; the worst case of rain intensity (WCI) and the worst case of rain return period (WCRP) of the *Gävleregnet* of 2021.

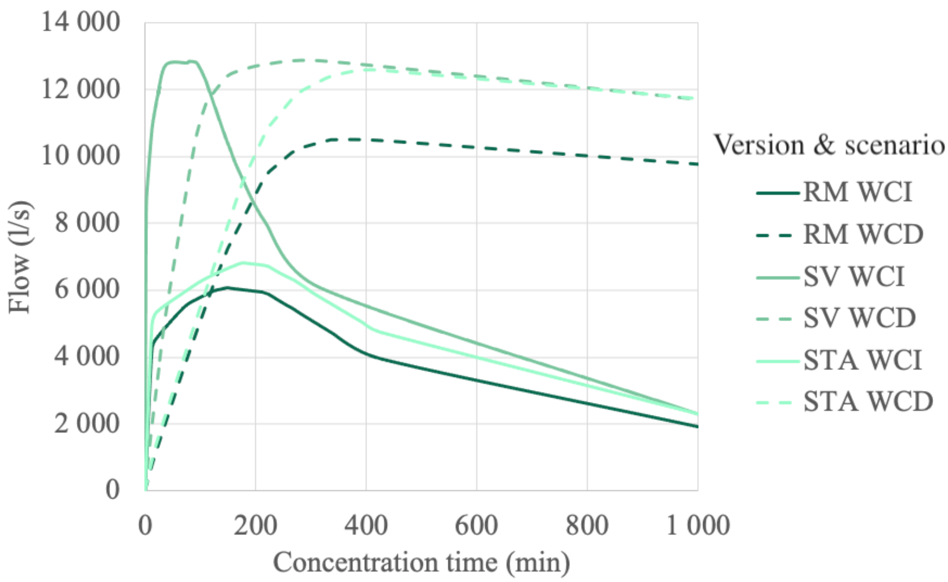

Figure 5.9: *The calculated water flows due to the heavy rainfall of August 17th in Brattfors, for both investigated rain scenarios, WCI and WCRP, as well as for the different calculation methods.*

As Figure 5.9 illustrates, the WCRP is the case in which the calculated flow is the highest for all investigated methods. It becomes evident that the peak flows are highest for the SV-RM method, and that the WCI for that particular method not only stands out in shape but also in peak value. The WCRP plots are similar for all three methods, but is noticeably lower for the RM compared to the other two. Furthermore, Table 5.10 below presents the calculated and dimensioning flows for the different methods and rain scenarios in Brattfors. The calculated flows refer to the peak flows visible in Figure 5.9 and the dimensioning flows are represented as the flows needed in Colebrook's method to give the calculated flows a (maximum) filling degree of 85% of the culvert pipe. This is only considered in the methods SV-RM and STA-RM.

Table 5.10: *The calculated peak flows presented in Figure 5.9, together with the corresponding dimensioning flows with regards to a filling degree of 85% of the culvert pipes.*

RM version	**Flow** (l/s)			
	Calculated		**Dimensioning**	
	WCI	**WCRP**	**WCI**	**WCRP**
RM	6 177	10 678	6 177	10 678
SV	12 846	12 875	15 113	15 147
STA	6 796	12 575	7 996	14 794

In Table 5.11, the calculated pipe dimensions in Brattfors for the different dimensioning flows of each calculation method and rain scenario are presented. The utilized Colebrook's diagram with regards to roughness are also presented, where the differences of the assumed roughnesses are due to specific regulations in the methods. In line with the results presented in Figure 5.9, the largest pipe dimensions are obtained for the rain scenario WCRP.

Table 5.11: *The needed pipe dimensions for the different calculation methods and rain scenarios in Brattfors*

RM version	**Colebrook's roughness** (mm)	**Pipe dimension** (mm) **WCI**	**WCRP**
RM	0.2	1 600	2 000
SV	0.2	>2 000	>2 000
STA	1.0	2 000	2 400

The flows in Vallsbo are presented in Figure 5.10 below. The results are presented for RM, SV-RM and STA-RM, as well as for the two rain scenarios, WCI and WCRP. Similar to the results for Brattfors in Figure 5.9, the highest peak flows are obtained for the WCRP scenario. The SV-RM method also reaches the highest peak for the WCI scenario. However, SV-RM the flows of a smaller magnitude compared to in Brattfors. Furthermore, the calculated and dimensioning flows in Vallsbo for each method and rain scenario are presented in Table 5.12 below.

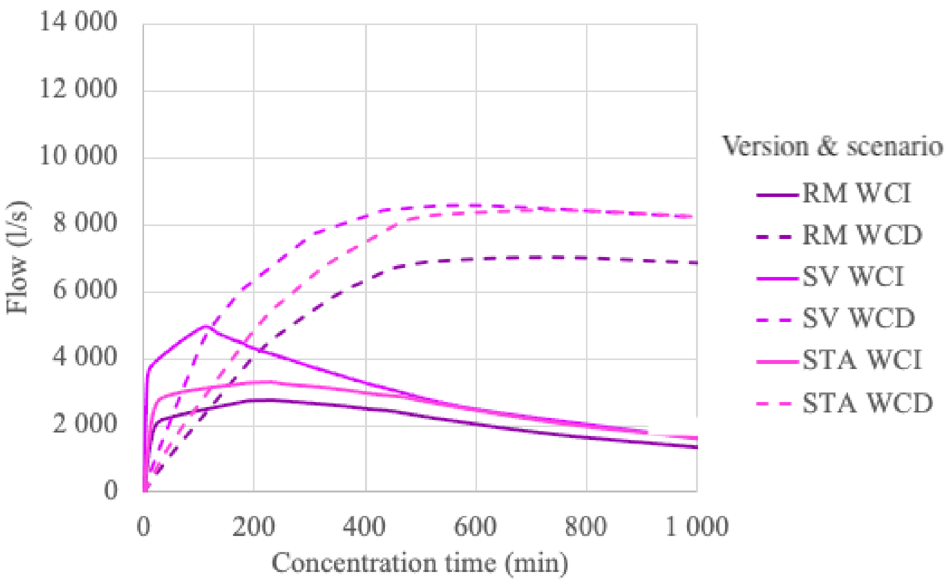

Figure 5.10: *The calculated water flows due to the heavy rainfall of August 17th in Vallsbo, for both investigated rain scenarios, WCI and WCRP, as well as for the different calculation methods.*

Table 5.12: *The calculated peak flows presented in Figure 5.10, together with the corresponding dimensioning flows with regards to a filling degree of 85% of the culvert pipes.*

RM version	Flow (l/s) Calculated		Dimensioning	
	WCI	**WCRP**	**WCI**	**WCRP**
RM	2 747	7 015	2 747	7 015
SV	4 926	8 564	5 796	9 663
STA	3 270	8 409	3 847	9 893

In Table 5.13 below, the required pipe dimensions in Vallsbo are presented for the different dimensioning flows of each calculation method and rain scenario. Since the pipe material for this case study is concrete, the same Colebrook's diagram was utilized for all investigated methods. This resulted in pipe dimensions varying between 1 400 mm and 2 000 mm at its greatest.

Table 5.13: *The needed pipe dimensions for the different calculation methods and rain scenarios in Vallsbo.*

RM version	Colebrook's roughness (mm)	Pipe dimension (mm) WCRP	WCRP
RM	1.0	1 400	1 800
SV	1.0	1 800	2 000
STA	1.0	1 400	2 000

5.6 Sensitivity analysis

The result of the sensitivity analysis for Brattfors are presented in Table 5.14 and Vallsbo in Table 5.15. The colours indicate the highest and lowest influenced parameter by each method and weather scenario, where green is the highest and red is the lowest. Also, to decide which investigated parameter that is most affected by the percentile change, the increased percentage has been divided by the percentile change. This makes a comparable percentile change per increased/decreased value. From the results it becomes apparent that all changes, positive or negative, give the same type of effect as the change, i.e. the positive changes give positive increases and the negative changes give negative increases. This is true for all investigated parameters, calculation methods and peak flows, except for Manning's coefficient in RM and STA-RM which do not consider Manning's coefficient to calculate their flows, since their flows are from tabulated values. There is also no apparent change of the peak flow in relation to the increased water velocity in the creek for SV-RM and the WCRP.

Table 5.14: *The percentage change and the percentile change per changed percentage of the peak flows for the investigated parameters in Brattfors, for each method and scenario. Green indicates the most influenced parameter and red the least.*

RM version	**Investigated parameters**	**Change** (%)	**Peak flow** WCI		WCRP	
				(%/%)		(%/%)
RM	Baseline (l/s)		6 068		10 498	
	Runoff coeff.	+100	+90%	0.90	+90%	0.90
	Water vel. Creek	+50	+15%	0.30	+2%	0.04
	Water vel. Land	+200	+55%	0.28	+2%	0.01
	Mannings coeff.	+50	±0%	0.00	±0%	0.00
	Catchment area	-62.5	-14%	0.22	-59%	0.95
SV	Baseline (l/s)		15 113		15 147	
	Runoff coeff.	+100	+91%	0.91	+90%	0.90
	Water vel. Creek	+50	+4%	0.08	±0%	0.00
	Water vel. Land	+200	+81%	0.41	+5%	0.02
	Mannings coeff.	+50	+46%	0.92	+2%	0.04
	Catchment area	-62.5	-12%	0.19	-60%	0.95
STA	Baseline (l/s)		7 996		14 794	
	Runoff coeff.	+100	+90%	0.90	+90%	0.90
	Water vel. Creek	+50	+12%	0.24	+1%	0.03
	Water vel. Land	+200	+49%	0.25	+2%	0.01
	Mannings coeff.	+50	±0%	0.00	±0%	0.00
	Catchment area	-62.5	-14%	0.22	-59%	0.95

Furthermore, the largest change of the results in Table 5.14 is recorded from the increase of the (forest) runoff coefficient to 200%, which gave a 91% increase of the peak flow for the WCI scenario in the SV-RM calculation method. But, the change of Manning's coefficient gave the largest percentile change per increased percent (0.92 %/%) for the SV-RM. For all calculation methods, the largest percentile change per increased percent is, however, obtained for the change of the catchment area in the WCRP scenario.

The result of the sensitivity analysis for Vallsbo are presented in Table 5.15, with the same color-coding are the as described for Table 5.14 above. The results for Vallsbo are similar to the results for Brattfors, where the largest increases are obtained by the increase of the runoff coefficient for all calculation methods. Also, the catchment area is still obtained as the parameter that changes the most in percent per increased percentage (0.93-0.98 %/%), for all calculation methods in the WCRP scenario.

Table 5.15: *The percentage change and the percentile change per changed percentage of the peak flows for the investigated parameters in Vallsbo, for each method and scenario. Green indicates the most influenced parameter and red the least.*

RM version	**Investigated parameters**	**Change (%)**	**Peak flow**			
			WCI		**WCRP**	
				(%/%)		(%/%)
RM	Baseline (l/s)		2 747		7 015	
	Runoff coeff.	+100	+90%	0.90	+92%	0.92
	Water vel. Creek	+50	+2%	0.04	±0%	0.00
	Water vel. Land	+200	+128%	0.64	+9%	0.05
	Mannings coeff.	+50	±0%	0.00	±0%	0.00
	Catchment area	-62.5	-11%	0.18	-58%	0.93
SV	Baseline (l/s)		5 796		9 663	
	Runoff coeff.	+100	+87%	0.87	+92%	0.92
	Water vel. Creek	+50	+1%	0.03	±0%	0.00
	Water vel. Land	+200	+144%	0.72	+3%	0.02
	Mannings coeff.	+50	+41%	0.82	±0%	0.00
	Catchment area	-62.5	-11%	0.17	-61%	0.98
STA	Baseline (l/s)		3 847		9 893	
	Runoff coeff.	+100	+88%	0.88	+92%	0.92
	Water vel. Creek	+50	+2%	0.04	±0%	0.00
	Water vel. Land	+200	+123%	0.62	+9%	0.05
	Mannings coeff.	+50	±0%	0.00	±0%	0.00
	Catchment area	-62.5	-11%	0.18	-58%	0.93

6
Discussion

In this chapter, the results of the thesis are further discussed and analysed in the following six sections. Section 6.1 covers the discussion of the results of areal parameters and runoff distances. The water velocity, the flows and the sensitivity analysis are analysed in Section 6.2, followed by Section 6.3 which discusses the resulting culvert pipe dimensions. Further discussion about weather data, climate and weather in general is found in Section 6.4. Sources of error are discussed in Section 6.5, and finally, further studies are presented in Section 6.6.

6.1 Areal results and runoff distances

One of the objectives of this thesis is to examine the differences between the manually preformed calculations and the results from the modelling in *Flödesappen.* Since the catchment areas for both case studies were larger than 100 ha, no flow could be calculated with the RM in the app, unfortunately. Moreover, as the app itself has not been developed enough to calculate the flow for rain with a return period as great as the ones studied in this thesis, the modelling has only been focused on the results of the comparable parameters; the areal parameters. The different included land covers are also compared, where *Flödesappen* in comparison to the manual approach takes more different types into consideration for assessment of runoff coefficients and areal percentages.

When comparing the results of the different areal parameters in Brattfors, shown in Table 5.2 and 5.6, it becomes evident that the sizes of the total catchments areas are similar in size, valued to 685 ha manually in GIS and 650 ha in *Flödesappen.* A notable difference is that the total catchment area retrieved in the app needed to be summarized to cover the runoff area all the way to the culvert pipe. This indeed can be seen as a source of error, but which is a pronounced development point at the time of writing, as described in Section 2.1.5.

In Table 5.3 and 5.7, the land covers in Brattfors estimated in GIS are indeed similar to the ones from *Flödesappen*, above all, that the largest proportion of the catchment area corresponds to forested land. However, one important difference is that *Flödesappen* makes it possible to separate the clear-felled areas from the forested land. Given that trees absorb water, it is thus not unreasonable to believe that clear-felled areas to some extent can result in an increased runoff compared to forested land, which makes a difference to the runoff coefficient. When it comes to the longest runoff distances, the path calculated in *Flödesappen* for part 3, is actually longer than the longest one calculated manually in GIS (see Table 5.2 and 5.6). This may be considered quite understandable due to the fact that the path calculated in *Flödesappen* manages to consider a more detailed extent of hydrographical flow lines compared to the manual calculations and approach in GIS.

Much like the case for Brattfors, the manually drawn total catchment area for Vallsbo was greater than the one processed by *Flödesappen*, only for Vallsbo, the percentile and valuable difference was much greater with measured catchments at 476 ha to 375 ha. Another likeness that indeed also is expected was that the longest runoff distance for *Flödesappen* was longer than the hand drawn one. When it comes to the land cover, a total of 82.8% was estimated to be covered in forests. When summarizing the land cover categories mentioned in Table 5.9, the total percentage that could be interpreted as forested land adds up to 95.6%, which indeed is a mentionable difference. Another noticeable part is that the exposed bedrock varies between 1.3% and 0.01%. Since the total catchment differs with about 100 ha, almost 20%, it is likely that some differences in land covering may be due to that.

6.2 Velocities, flows and sensitivity

The calculated water velocities that are presented in Figure 5.8 are much greater than the measured ones, that are plotted in the same figure. The reason for this is that the calculated flows are for the *Gävleregnet* and the once measured in field are for a normal to slightly higher normal flow. The figure shows that the calculated velocities indeed are greater, but since they are supposed to represent a rain with a return period of 3 900 years, they might be reasonable. When dimensioning a culvert pipe, a velocity inside these should not exceed 1.5-2 m/s (A. Gunnarsson, personal communication, May 20th 2022) since too extensive erosion barriers might then be needed. Therefore, a velocity of about 3 m/s during such a rain, might be plausible.

What can be further seen in Figure 5.8 is that the spread of results in Brattfors are greater than in Vallsbo. This might be due to the fact that there are more watercourses in Brattfors and that they are located in a more varied terrain than in Vallsbo. But as mentioned in Section 5.2.1, it is possible that some profiles might have been placed alongside the creeks instead of exactly in the creek, which indeed may have affected the gradient of certain runoff areas.

In Figure 5.9 and 5.10 the calculated flows for the two case studies are presented. As can be seen, the greatest flows are obtained for WCRP for both case studies. The values for these can be seen in Tables 5.10 and 5.12, where the calculated peak flows are presented. When comparing the plots between each other it becomes apparent that the greater flows are in Brattfors, which indeed seems likely due to the fact that its catchment area is bigger than Vallsbo.

The flow estimated for SV-RM and WCI in Brattfors, see Figure 5.9, has an interesting peak that can be explained by the factors of which the flow is dependent. The climate factor, the reduced area but mostly by the rain intensity. Since the weather scenario, WCI, indeed has a great intensity, see Figure 4.3. The reduced area is in that way not as decisive for the total flow as the intensity is during the first minutes of the rain event. This is due to its initial greatness of intensity, but since the intensity decreases much more and much faster than the WCRP scenario, the reduced area becomes more important. The oddly shaped peak appeared due to the fact that the reduced area is thus rising as fast as the rain intensity is dropping.

In Section 2.1.1, it was highlighted that the Rational Method (RM) is surface size dependent as it is less suitable for larger catchment areas over a certain limit. However, this limit is defined differently by different sources and is therefore not explicitly determined. For example, as also mentioned earlier, the RM should not be applied to catchment areas over 80 ha according to Chin (2018). But on the contrary, SV (2016) states the importance of utilizing the Time-area method (T-A) for catchment areas larger than 20-30 ha, which is a significantly lower limit. Therefore, the extent to which subdivisions of the catchment area had an effect on the result of the calculated peak flows was investigated in the sensitivity analysis (SA). In Table 5.14 and 5.15, this effect is depicted by a negative percentile change of each sub-area with 62.5%, corresponding to a change in the maximum permitted sub-areas from 80 ha to 30 ha. For each rain scenario, it can be seen to give a relatively even reduction of the peak flows for all three calculation methods, varying between 11-14% and 58-61% in total for both case studies.

A probable reason for this even result in the SA may be that the reduction of the sub-areas was only applied as a percentile change without taking into account that the same total catchment area is maintained. The most optimal reduction would have been to re-do the sub-division of the total catchment area so that it instead was divided into an additional number and smaller areas, but unfortunately that would have been too time consuming and too big of a scope for a SA in this thesis.

In Section 2.1.1, it was also highlighted that the RM is an estimation method primarily applied to more or less impervious surfaces in urban areas. The areas in this thesis mainly are rural, which of course is the opposite to this, but as the aim clarifies, this was disregarded to investigate the methods possibilities. Since the runoff coefficients are developed for the RM it is possible that the factors are not as suitable for rural areas alike. During the theory study it became evident that Young et al. (2009) and Wong (2002) both doubts the reliability of the runoff coefficients even for the RM. This of course instituted the factor as a good sensibility parameter. The runoff coefficient for land was increased by 100% from 0.1 to 0.2 with indeed affected the peak flows for all of the calculation method and rain scenarios. The greatest increase in peak flow seems to be for Vallsbo and the scenario of worst case of return period (see Table 5.14 and 5.15).

The SA shows that an increased velocity in the creek does not affect the peak flow for worst case of return period (see Table 5.14 and 5.15). This is probably due to that the intensity of the rain is closer to constant during the whole event, compared to the intensity in for worst intensity scenario. This can be seen in Figure 4.3, where it becomes obvious that the worst intensity varies between about 1 000 to 10 l/(s · ha), while the worst duration varies between 200 and 100 l/(s · ha). This further means that the reduced area has greater significance for the flow and variation in flow for the worst intensity scenario then the worst duration scenario.

What also can be stated from the SA is that the change in the velocity in the creek does not affect the peak flows in SV-RM as clearly as in RM and STA-RM. But a factor that increases the flow for SV-RM is the change in Manning's coefficient, which indirect changes the water velocity and thereby the peak flow. Manning's equation was only utilized in SV-RM to calculate the water velocities, and in this thesis, it was done for all of the different runoff surfaces. A possible reason why Manning's coefficient in SA gave a greater result than only the increase of the water velocity, might be that the velocity in the creeks is not the dominating factor, but the water velocity flowing on land is. When regarding the increased percentile change of peak flow calculated for SV-RM and velocity on land, the increase of 200% gave an 81% higher peak flow for Brattfors and 144% for Vallsbo.

Even though some percentages presented in Table 5.14 and 5.15 might seem impressive, it is important to remember that all the investigated parameters are increased or decreased with a certain percentage. For example, the impressive change of 144% of the Water velocity on land in Vallsbo for SV-RM and WCI might appear to give the most increased flow. But, when compared to the percentile change of the investigated parameter, it does not. Instead, as mentioned in Section 5.6, the most affected flow is generated by the change of the catchment area for SV-RM and WCRP, which is seen to affect the result with 0.98 percentage per percentage of change.

As stated above, when regarding Table 5.14 and 5.15 in the SA, it can be seen that Manning's coefficient and the runoff coefficient have a big impact on the results. To make the model more accurate, these parameters could be adapted by examine them more closely in field and let them vary in the model. This is a concrete example on how the field visit could have affected the results and thereby the sensitivity analysis.

When regarding Table 5.14 and 5.15 in the SA, it can be seen that Manning's coefficient and the runoff coefficient have a big impact on the result. To make the model more accurate, these parameters could be adapted by examine them more closely in field and let them vary in the model. This is a concrete example on how the field visit could have affected the results and thereby the sensitivity analysis.

6.3 Dimensions of culvert pipes

The required pipe sizes for the two case studies were presented in Tables 5.11 and 5.13. As mentioned in the terminology, pipes with a dimension greater than 2 000 mm are regarded as bridges. This makes the greatest proposed pipe dimensions in Brattfors just that, bridges. For Brattfors, the pipe dimensions varied between 1 600 and 2 400 mm. The location at the time of the incident was fitted with a 1 600 mm steel pipe, after the rain incident, it was refitted with a 1 900 mm trenchcoat pipe. In Vallsbo, the dimensions varied between 1 400 and 2 000 mm, which is at least 200 mm greater than the current pipe.

During the dimensioning with Colebrook, two different roughness factors were utilized in the Brattfors case, due to the different regulations and guidelines in the different methods. The STA for instance advises its readers to only utilize 1.0 mm roughness diagram, at the finest. But since the trenchcoat has a plastic lining, the authors utilised the 0.2 mm diagram, which indeed could have affected the results to the less conservative side. Another characteristic of the trenchcoat pipe is that it is corrugated. This corrugation is however not mentioned to affect the result or alter the need for any type of roughness in relation to the Colebrook's diagrams according to Young et al. (2009) and Wong (2002).

Since the pipe sizes required to handle the dimensioning flow actually were not that incredibly great, the pipe break in Brattfors might be due to other causes then water pressure. Possible factors causing this can have been that the inclination and position of the culvert pipe in Brattfors were not ideal, or that there was a lack of sufficient shallow depth in the pipe. According to the STA (2021a), water-carrying culvert pipes must be provided with shallow depths, both to facilitate fauna passage but also to prevent water flowing along the pipe on its outside. If water seeped in along the outside of the pipe, this might have caused a lack of bearing capacity, especially if the surrounding material was of finer friction soils, such as sand. In this case, due to the location, the small traffic load and the location's surrounding soil materials, it is feasible that sand was used in the embankment.

During the field visit on both of the sites, it became evident that both locations are equipped with protections against erosion. In Brattfors there was crossed rock strewn along the inlet and outlet of the pipe. In Vallsbo, there was a stone wall on each side of the inlet, to direct the water though it.

6.4 Weather and climate

The rain data that was utilized for the calculations in this report were actually data retrieved and analysed for Gävle, although the applied case studies both are located in Ockelbo. This is due to the close location between the city and the town (see Figure 3.1) and also the availability of processed data. It is known that weather indeed is really changeable (Buishand, 1991), and although it is raining on one side of town, it could be blazing on the other, which of course is a source of error for this study. Worth mentioning also, is that the data was analysed for Gävle, but by utilizing the station-year method, which indeed utilizes material from measuring stations in relatively near location. This makes the validity of the data more profound.

The *Gävleregnet* of 2021, indeed was a very heavy rainfall. As presented in Figure 3.8 and 3.9, the precipitation of the month of August was almost 300% of expected, compared to the new normal values of 1991-2020 and the southern parts of Gävleborg. What also is presented in Figure 3.8, is that many of the stations plotted, already had received the normal amount of precipitation for the whole month, the day of the rain event. This can be an indication that the soil was already saturated during the rainfall. When considering Figure 3.9, it becomes apparent that the month leading up to August, July, actually had less rain volume than normal. This knowledge together with the knowledge that the summer months generally is the months in which the water bodies are drained, may contradict that the soil was moisture saturated. Another statement that can support the assumption about moisture saturation is that soil can not absorb to their full potential during full rain with large intensities or long durations.

This report has assumed that the soil is saturated with moisture, which was based on the claim that so much rain had come during the two weeks leading up to the studied rain event. The sensitivity of the runoff velocity on land was therefore analysed in the SA and it was presented that the peak flow increased up to the impressive 144% at the most, in Vallsbo for SV-RM and the WCI scenario.

The method that was used to retrieve the rain return periods was the station-year method. The method in itself is sensitive to utilizing of data in which the collecting stations are situated too close to one another, since each station is supposed to count as a stand-alone/statistically independent (Buishand, 1991). It is also known to be less reliable during extreme weather analyses (SMHI, 2017). To make the data more reliable, the Swedish Meteorological and Hydrological Institute (SMHI) removed the outliers of the data set to make the estimation more accurate (SMHI, 2021a). And as mentioned in Section 3.3, the highest measurements of precipitation that this report is based on is thus not included in the prediction of the return period. The provided data actually also included return periods calculated in three different methods, and the SMHI (2021a) thought that the Station-year method was the method that best reflected the type of return period that the rain actually inhabited. Since the authors does not possess the knowledge of weather estimations, it was decided to assume return periods in line with those recommended by SMHI. However, since the data included rain measurements that could be transformed into a rain intensity, the return period was not utilized in any calculations.

In P110, the importance of being updated on the actual state of knowledge about climate assessments is emphasized as continued effects of climate change emerge (SV, 2016). The discussion about climate change scenarios including heavier precipitation in Sweden, is oftentimes bought up. It is important to understand that even if *Gävleregnet* was extraordinary, similar rain events most likely already have happened in Sweden. Just on locations where the event was not recorded or any significant infrastructure damaged. If a specific rain with a specific return period actually reoccurs more often, the statistical estimation method is not accurate. But there are other uncertainties also. Th Swedish Council of Experts on Climate Adaptation (2022) says that a majority of the Swedish municipalities utilities different climate scenarios and simulated times, and the council agrees with the statement that the information is disseminated and needs to be collected and structured. SMHI (2015a) mentioned that during the development of a climate scenario there are several factors of uncertainty, like the natural variation of the climate, the models' uncertainties and also the future emissions of greenhouse gases. The climate scenarios are often related to as RCP, which is the foundation for the development of climate factors. The values for the climate factors according to the assessed climate scenarios by SV-RM were presented in Table 2.4 and 2.5, where the factors are estimated for precipitation with a 10 year return period. Unfortunately, 10 year indeed is a low return period, and during the extrapolation to 100 years the insecurity of the factors increases and should only be considered as an approximation (SMHI, 2015b). According to SMHI (2015b), the percentile difference between the extrapolated 100 year precipitation and the original 10 year only differs with about 1%.

6.5 General sources of error

During the work with this master thesis, a number of sources of error were identified. It has generally been challenging to interpret the guiding documents and find the most appropriate data and approach for the used methods. Parts of the work in this thesis thus needed to be based on assumptions. And many, if not all, of these assumptions are related to the nature/character of the catchment area, as it is the basis for area-specific input data vital for the calculation and evaluation process.

Nature is so incredibly complex and involves an enormous number of factors and processes that in one way or another are dependent on and affect each other. Seeing and analysing nature with the help of different maps can therefore give a limited picture of reality. Of course, today there is much more advanced technology and access to digital modelling tools that can provide a more comprehensive analysis in several dimensions, in comparison with traditional analyses of graphic maps and two-dimensional data. But no matter how good technology and data are available it is a fact that depictions of nature will never truly correspond to reality due to its complexity, which thus requires assessments and various assumptions to be made. This emphasizes the importance of performing site analyses through field visits as a complement to investigations and modelling digitally.

During the performed field visit, a few water velocities were measures according to the orange method. The method was selected due to its simplicity and since its accuracy was regarded as acceptable for the cause. During the process of measuring the water velocity, it became evident that some errors in this very simple method indeed did occur. One of these being that the recorded time for the orange to flow a certain distance was overestimated, implying that the measured water velocities might be greater than presented. This is due to the measurement technique when the orange was dropped into the water, ever so slightly and close to the surface, it was lowered below the surface before it floated up to the surface and then went with the water. This error is likely to affect the measurements with shorter duration more than the longer recorded. Another error that always should be mentioned in relation to method like this is the human factor, which indicates the reaction time of the person timing.

Furthermore, the time factor during the field visit played a decisive role in the number of hydrographic and area-specific observations that could be made within the catchment areas. Observations from the visited places were thus assumed to be representative for all other such places identified in the GIS-maps, which indeed is a simplification of the reality that implies uncertainties in the results. However, with regard to the discussion above, it can be assumed that such uncertainties would have become even greater if the field visit had not taken place at all. The assumptions could then not have been based on actual perceived observations, which can be assumed to have a significantly greater chance of also agreeing with more places in the immediate area than the otherwise map-based guesses. This can also be underlined by the results of the estimated boundaries of the catchment areas in Figure 5.2a and 5.2b. Although no calculations were made at the initial assessment, some clear differences can be distinguished by only looking at the shapes of the areas assessed before compared to after the field visit.

As mentioned in Section 2.1.1, the RM includes a lot of assumptions. The constant ratio between the runoff and the rainfall is one such assumption, which also presupposes that the precipitation intensity is constant and that the rain duration either reaches or exceeds the concentration time of the catchment area (Chin, 2018). This of course is a rough simplification of the reality, since neither rainfall nor runoff is naturally constant over the concentration time, which Chin (2018) claim to underestimate the maximum runoff rate. In other words, the method does not take into account the spatial variation of the precipitation rate that exists within a catchment area, which according to both Chin (2018) and Lyngfelt (1981) is a significant uncertainty especially for larger catchment areas. Nor does it consider any explicit infiltration capacity for permeable land covers, other than indirectly as rainfall abstractions are integrated in the runoff coefficient. As no other methods have been studied, it is therefore difficult to conclude the trustworthiness of the calculated results.

The methods utilized in this thesis does not consider a background flow in creeks during the dimensioning process. It is likely that the background flow as well as the dimensioning flow of a year-specific rain fall will increase due to climate change, this may result in the need of a dimensioning method that includes a background flow. Much like the lack of regard for background flow, the methods do not consider the process of *gaining stream*, which indeed might increase the flow at a point of outflow. The value of a gaining stream flow is hard to assess, due to a wide range of different factors contributing.

Important to mention is that the applications of the RM utilized in this report are indeed estimation methods. Some insecurities will be present no matter how carefully they are selected, therefore sometimes, to refine some parameters will not change the accuracy of the result. Some sources of error could thus be seen as necessary or even beneficial for such a method to make it fast and easy to use, which, for example, is desirable when dimensioning a single culvert pipe on a road with low traffic load, located in a rural and sparsely populated area.

6.6 Further studies

During the work with this master thesis, the authors needed to narrow down the scope of the report a few times, given the assumptions made. Below are some ideas that might be a good starting point for coming master theses or other academic papers within the subject.

One factor that were found to be sought after in the industry and always made experienced engineers excited was to study the water velocity. This thesis calculated own water velocities dependent on the Manning's equation, but also utilized tabulated values. These values are referred to in many sources, but where och how they were developed, and how well they correspond to reality nowadays, are not really given. Therefore, a study of water velocities in relation to different land covers and inclinations of the terrain indeed would be of interest. Especially, further studies of the effect that clear-felled areas have on the runoff and its velocity.

Another idea, related to the calculations of water velocity, would be to investigate and tabulate different Manning's coefficient for different types of land cover and inclinations.

7 Conclusion

Following conclusions of the thesis and its defined research questions are made:

- **What were the estimated maximum peak flows of *Gävleregnet* in August 2021 for the two case studies, and what pipe dimensions were desired to manage these flows?**

The maximum peak flow of rainwater runoff during the extreme rainfall event of August 2021 event in Gävleborg county was estimated to 12 875 l/s and 8 564 l/s in Brattfors and Vallsbo respectively, which both were based on the scenario for worst case of return period (WCRP), and are scaled up to represent a pipe with an 85% degree of filling. The flow for Brattfors was given by using the application of the Rational Method (RM) according to Svenskt Vatten (SV), whereas the flow in Vallsbo was retrieved by the variant according to The Swedish Transport Administration (STA). However, in Vallsbo, the maximum flow was only marginally larger for STA-RM than for SV-RM, barely discernible in the generated flow diagrams. The culvert pipe dimensions needed for the maximum flows and rain scenario corresponded to >2 000 mm in Brattfors and 2 000 mm in Vallsbo. Hence, a culvert pipe of maximum size is therefore sufficient for Vallsbo, but since the dimension in Brattfors exceeds 2 000 mm, a bridge is required there.

- **According to the sensitivity analysis, which parameters have the largest impact on the calculated results?**

The thesis investigates the influence that five different parameters had on the resulting peak flow for the two case studies and the two rain scenarios. The parameter that was deemed as the most affecting for both of the case studies was the size of the catchment area for the WCRP scenario. The second most influential parameter was the runoff coefficient for the woodlands, the results were high for both case studies and weather scenarios. The least affecting parameter apart from the Manning's coefficient for RM and STA-RM, was the water velocity in the creek for the WCRP. For Vallsbo, even the water velocity on land was among the least affecting ones.

Outside the scope of the research questions, it is highlighted that RM known to be a rough estimation suitable for stormwater calculations in urban areas. Within this thesis, the RM and some of its variants have been applied to estimate rainwater runoff for two rural case studies which mainly consist of natural land. This was done in order to investigate if the method still could give an acceptable estimation despite its limitations. And as a result, this report wants to highlight the limitations and assumptions that can be made for these kinds of analyses. There are also a lot of uncertainties related to the RM and its applications, especially when it comes to assumptions of nature and weather conditions, and it is difficult to determine what direct impact these have on the results. It is thus important to also remember the purpose of a rough estimation method, which is literally as it phrases; a method for *rough estimations.*

Finally, the authors would like to emphasize the importance of actually visiting the case study areas. As mentioned in the discussion, the assessment of the areas varied much between before and after the field executed visit. The result would thus have been less reality-based if the field visit had been excluded.

Bibliography

Andersson-Sköld, Y., Nordin, L., Nyberg, E., and Johannesson, M. (2021). A framework for identification, assessment and prioritization of climate change adaptation measures for roads and railways. https://doi.org/10.3390/ijerph182312314.

ASFT Industry AB (n.d.). Precipitation sensor – optic eye™. https://www.sarsys-asft.com/optic-eye. Retrieved: 2022-03-15.

Bondelind, M. and Häggström, S. (2018). *Hydraulik : för samhällsbyggnad*. Liber.

Brkić, D. (2011). Review of explicit approximations to the colebrook relation for flow friction. https://doi.org/10.1016/j.petrol.2011.02.006.

Buishand, T. A. (1991). Extreme rainfall estimation by combining data from several sites. https://doi.org/10.1080/02626669109492519.

Chin, D. A. (2018). Estimating peak runoff rates using the rational method. https://doi.org/10.1061/(ASCE)IR.1943-4774.0001387.

County Administration of Örebro (2003). https://www.lansstyrelsen.se/download/18.11a2cbf716d6c8f9f7415270/1571661327956/Att_anlagga_vagtrummor.pdf. Retrieved: 2022-06-08.

Dahlström, B. (2006). Regnintensitet i sverige – en klimatologisk analys. http://vav.griffel.net/filer/VA-Forsk_2006-26.pdf. VA-forsknings rapport Nr 2006-26.

Dahlström, B. (2010). Regnintensitet – en molnfysikalisk betraktelse. http://vav.griffel.net/filer/Rapport_2010-05.pdf. Rapport Nr 2010–05.

Dhakal, N., Fang, X., Asquith, W., Cleveland, T., and Thompson, D. (2013). Rate-based estimation of the runoff coefficients for selected watersheds in texas. https://doi.org/10.1061/(ASCE)HE.1943-5584.0000753.

Jonsson, J. (2019). Nästa generations vvis. https://docplayer.se/190043743-Nasta-generations-vvis-jonas-jonsson-nationell-samordnare-vvis-tmall-0145-presentation-widescreen-v-1-0.html. [PowerPoint Presentation].

Jonsson, J. (2020). Jämförelse av väderobservationer vvis ms4 - ms7. https://www.trafikverket.se/contentassets/9d8e72bc0c904a9da77abec06d7583c2/rapport-vvis-ms7-vaderobservationer-vid-oat---kort-1.0.pdf.

Lindeberg, G. (2020). Flödesberäkningar. [Not published].

Lindeberg, G., Wiman, S., and Hård, J. (2019). Flödesapplikation. [Not published].

Lyngfelt, S. (1981). Dimensionering av dagvattensystem rationella metoden. https://publications.lib.chalmers.se/records/fulltext/179020/local_179020.pdf.

MSB (2021). Översvämningarna i gävle 2021. https://www.msb.se/sv/aktuellt/avslutade-handelser-och-insatser/oversvamningarna-i-gavle/. Retrieved: 2022-03-04.

National Swedish Land Survey (n.d.). Min karta. https://minkarta.lantmateriet.se. Retrieved: 2022-06-08.

P4 Gävleborg/Sveriges Radio (2021). Två veckors omväg väntar för jädraåsborna. https://sverigesradio.se/artikel/tva-veckors-omvag-att-vanta-for-jaderforsborna. Retrieved: 2022-03-04.

Sabzevari, T. (2017). Runoff prediction in ungauged catchments using the gamma dimensionless time-area method. https://doi.org/10.1007/s12517-017-2852-0.

SGU (nd). Jordarter 1:1 miljon. https://apps.sgu.se/kartvisare/kartvisare-jordarter-1-miljon.html. Retrieved: 2022-03-04.

SLU (2014). Att räkna på vatten – en formelsamling för landskapsingenjörer. https://pub.epsilon.slu.se/11781/11/persson_j_etal_150203.pdf. Rapport 2014:17.

SMHI (2009). Korttidsnederbörd i sverige 1995 - 2008. https://www.smhi.se/publikationer/publikationer/korttidsnederbord-i-sverige-1995-2008-1.10136. FAKTABLAD NR 43 – 2010.

SMHI (2015a). Framtidsklimat i gävleborgs län - enligt rcp-scenarier. https://www.smhi.se/polopoly_fs/1.165070!/Klimatologi_36%20Framtidsklimat%20i%20Gävleborgs%20län%20-%20enligt%20RCP-scenarier.pdf. KLIMATOLOGI Nr 36, 2015.

SMHI (2015b). Sveriges framtida klimat. https://www.smhi.se/polopoly_fs/1.165048!/Klimatologi_14%20Sveriges%20framtida%20klimat%20-%20Underlag%20till%20Dricksvattenutredningen.pdf. KLIMATOLOGI Nr 14, 2015.

SMHI (2017). Extremregn i nuvarande och framtida klimat - analyser av observationer och framtidsscenarier. https://www.smhi.se/polopoly_fs/1.165084!/Klimatologi_47%20Extremregn%20i%20nuvarande%20och%20framtida%20klimat%20Analyser%20av%20observationer%20och%20framtidsscenarier.pdf. KLIMATOLOGI Nr 47, 2017.

SMHI (2021a). Analys av gävleregnet augusti 2021. [Not published].

SMHI (2021b). Dataserier med normalvärden för perioden 1991-2020. https://www.smhi.se/data/meteorologi/dataserier-med-normalvarden-for-perioden-1991-2020-1.167775.

SMHI (2021c). Svenska nederbördsrekord. https://www.smhi.se/kunskapsbanken/meteorologi/nederbord/svenska-nederbordsrekord-1.6660. Retrieved: 2022-06-08.

SMHI (n.d.a). Ladda ner meteorologiska observationer. https://www.smhi.se/data/meteorologi/ladda-ner-meteorologiska-observationer/#param=precipitation24HourSum,stations=all. Retrieved: 2022-04-14.

SMHI (n.d.b). Månads-, årstids- och årskartor. https://www.smhi.se/data/meteorologi/kartor/avvikelse/manadsnederbord-procent-av-normal-avvikelse/manad/april. Retrieved: 2022-04-01.

STA (2016). Slutrapport - förstudie indra 2016. https://www.trafikverket.se/contentassets/9d8e72bc0c904a9da77abec06d7583c2/study-indra-2020---svenska---swedish.pdf.

STA (2017). Avvattningsteknisk dimensionering och utformning - mb 310. https://trvdokument.trafikverket.se/Versioner.aspx?spid=3583&dokumentId=TDOK%202014%3a0051. TDOK2014:0051.

STA (2019). A framework for identification, assessment and prioritization of climate change adaptation measures for roads and railways. https://doi.org/10.3390/ijerph182312314.

STA (2021a). Avvattning - avvattning, dimensionering och utformning. https://puben.trafikverket.se/dpub/visa-dokument/cf9d5277-b5e2-461b-a968-0add893e23ba. TRVINFRA-00231.

STA (2021b). Vägtrafikflödeskartan. http://vtf.trafikverket.se/SeTrafikinformation. Retrieved: 2022-03-09.

STA (n.d.a). Flödesapp. https://flöde.se. Retrieved: 2022-06-03.

STA (n.d.b). Trafikverkets väderinformation vvis. https://www.trafikverket.se/tjanster/trafiktjanster/VViS/. Retrieved: 2022-02-21.

STA (n.d.c). Vägväderinformationssystem, vvis. https://trafikverket.ineko.se/se/v%C3%A4gv%C3%A4derinformationssystem-vvis. Retrieved: 2022-02-21.

SV (2016). P110 del 1 och 2: Avledning av dag-, drän- och spillvatten - funktionskrav, hydraulisk dimensionering och utformning av allmänna avloppssystem. ISSN: 1651-4947.

SVT (2021). Skyfallet över gävleborg slår historiska rekord. https://www.svt.se/nyheter/lokalt/gavleborg/skyfallet-over-gavleborg-slar-historiska-rekord. Retrieved: 2022-03-04.

Swedish Council of Experts on Climate Adaptation (2022). Första rapporten från nationella expertrådet för klimatanpassning. https://klimatanpassningsradet.se/polopoly_fs/1.180289!/Rapport%20från%20Nationella%20expertrådet%20för%20klimatanpassning%202022.pdf.

Vaisala (2018). Present weather and visibility sensors pwd10, pwd12, pwd20, and pwd22. https://www.vaisala.com/sites/default/files/documents/PWD-Series-Datasheet-B210385EN.pdf. Retrieved: 2022-03-15.

Wong, T. S. W. (2002). Call for awakenings in storm drainage design. https://doi.org/10.1061/(ASCE)1084-0699(2002)7:1(1).

WWF (n.d.). Mäta vattenflöde. https://www.wwf.se/utbildning/uppgiftsbanken/mata-vattenflode/. Retrieved: 2022-05-06.

Young, C. B., McEnroe, B. M., and Rome, A. C. (2009). Empirical determination of rational method runoff coefficients. https://doi.org/10.1061/(ASCE)HE.1943-5584.0000114.

A
Colebrook's diagrams

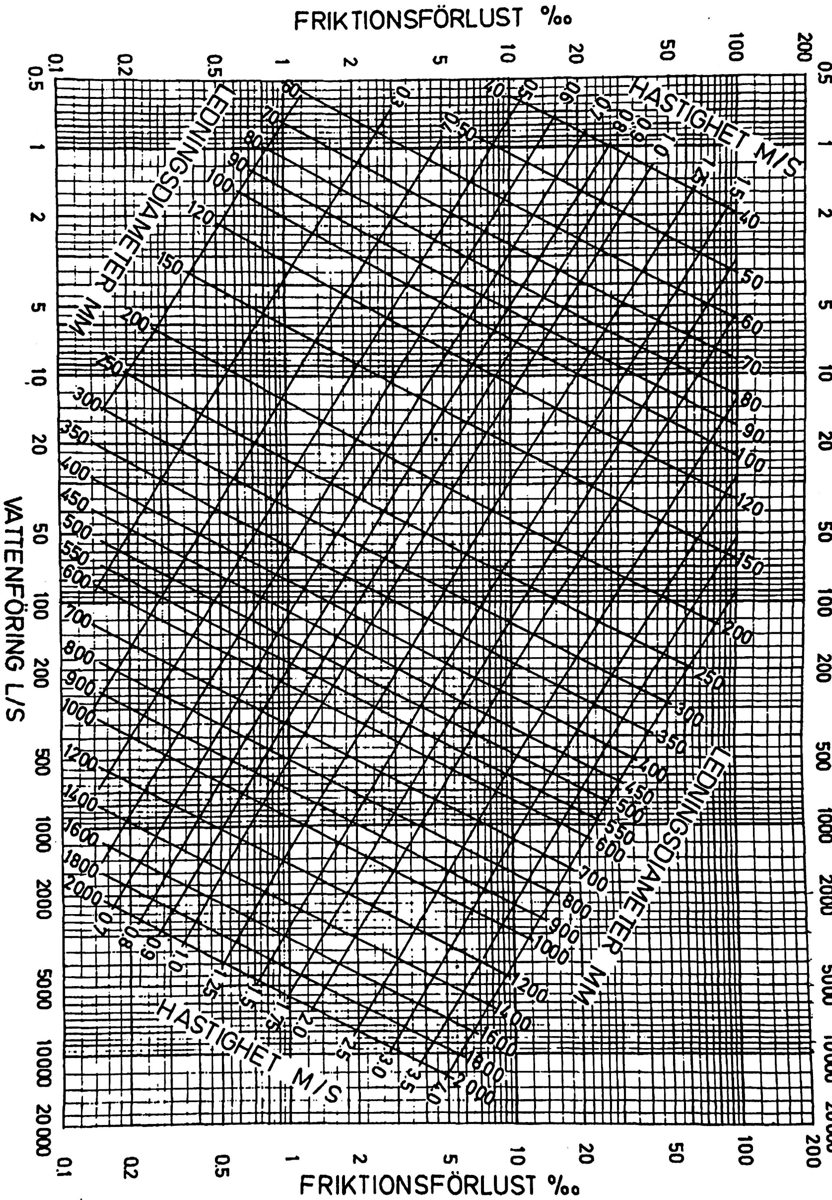

Figure A.1: *Colebook's diagram for roughness k = 0.2 mm (SV, 2016). Translation: "Vattenföring L/S" = Flow (l/s), "Friktionsförlust ‰" = Pipe gradient (‰), "Ledningsdiameter MM" = Pipe dimension (mm) and "Hastighet M/S" = Water velocity (m/s)*

B
Unit conversion

In the following Equation B.1, the precipitation unit of millimeters, which indicates millimeters per hour, is converted into the rain intensity unit of $l/(s \cdot ha)$. The equation clarifies that a factor of $10^4/3600$ can be multiplied to a precipitation per hour to transform that value into a rain intensity.

$$
\begin{aligned}
mm &= \\
&= \frac{mm}{h} = \frac{mm}{h} \cdot \left(\frac{m^2}{m^2}\right) = \frac{10^{-3} \cdot m^3}{m^2 \cdot h} = \\
&= \frac{10^{-3} \cdot m^3}{m^2 \cdot h} \cdot \left(\frac{10^4 \cdot m^2}{ha}\right) = \frac{10 \cdot m^3}{ha \cdot h} = \\
&= \frac{10 \cdot m^3}{ha \cdot h} \cdot \left(\frac{10^3 \cdot l}{m^3}\right) = \frac{10^4 \cdot l}{ha \cdot h} = \\
&= \frac{10^4 \cdot l}{ha \cdot h} \cdot \left(\frac{h}{3600 \cdot s}\right) = \frac{10^4 \cdot l}{3600 \cdot s \cdot ha} = \\
&= \frac{10^4}{3600} \cdot \frac{l}{s \cdot ha}
\end{aligned}
\tag{B.1}
$$